Two-Color Two-Photon Microscopy

Von der Fakultät für Lebenswissenschaften

der Technischen Universität Carolo-Wilhelmina

zu Braunschweig

zur Erlangung des Grades eines

Doktors der Naturwissenschaften

(Dr. rer. nat.)

genehmigte

D i s s e r t a t i o n

von Stefan Quentmeier

aus Salzgitter

1. Referent:	Professor Dr. Karl-Heinz Gericke
2. Referent:	Professor Dr. Peter Jomo Walla
eingereicht am:	26.11.2008
mündliche Prüfung (Disputation) am:	22.12.2008

Druckjahr 2009

Vorveröffentlichungen der Dissertation

Teilergebnisse aus dieser Arbeit wurden mit Genehmigung der Fakultät für Lebenswissenschaften, vertreten durch den Mentor der Arbeit, in folgenden Beiträgen vorab veröffentlicht:

Publikationen

[1] S. Quentmeier, S. Denicke, J.-E. Ehlers, R. A. Niesner, K.-H. Gericke: Two-Color Two-Photon Excitation Using Femtosecond Laser Pulses. Journal of Physical Chemistry B 112: 5768-5773 (2008).

[2] S. Quentmeier, C. C. Quentmeier, P. J. Walla, K.-H. Gericke: Two-Color Two-Photon excitation of intrinsic protein fluorescence: a label free observation of a proteolytic digestion of BSA. ChemPhysChem, 2009 Jan 20. [Epub ahead of print]

[3] S. Quentmeier, S. Denicke, K.-H. Gericke: Two-Color Two-Photon Fluorescence Laser Scanning Microscopy. Journal of Fluorescence, accepted Mai 2009

Tagungsbeiträge

[1] S. Quentmeier, R. A. Niesner, K.-H. Gericke: Two-Color-Two Photon Excitation (2c2p). (Poster), Jahrestagung der Deutschen Physikalischen Gesellschaft (DPG), Regensburg (2007)

[2] J.-E. Ehlers, S. Quentmeier, R. Niesner, K.-H. Gericke: Two-Color Two-Photon Excitation (2c2p). PhotonsLive, Saarbrücken (2007)

[3] S. Quentmeier, C.C.Quentmeier, S. Denicke, J.-E. Ehlers, P.J. Walla, K.-H. Gericke: Monitoring Protein Digestion without labeling by using Time Resolved Two-Color Two-Photon Excitation. (Poster) Microscience, London (2008)

[4] S. Quentmeier, S. Denicke, J.-E. Ehlers, K.-H. Gericke: Two-Color Two-Photon Microscopy (2c2pLSM), Microscience, London (2008)

[5] K.-H. Gericke: Two-Color-Two-Photon Microscopy – imaging the intrinsic protein fluorescence. (Talk) Molec, St. Petersburg, (2008)

Content

1 Introduction

1.1 Microscopy

Over centuries, the classical optical microscope was the only tool that provided researchers images behind the limits defined by their eyes. During the last century light microscopy went through a tremendous development. But the basic idea of a lens or a set of lenses enlarging a reflective or transmitive image and making it visible to the eye of the viewer remained. Today, light microscopy shows a vast variety of different techniques. On the one hand, the classical light microscopy has been refined by additional contrast enhancing techniques. On the other hand, a complete new field of light microscopy has been established: the fluorescence microscopy. Here, the sample is excited to emit fluorescence light. Manipulating the excitation light and analyzing the emission light offers new ways of obtaining information about the often specifically prepared sample. This thesis deals mainly with a new way of excitation in fluorescence microscopy: the two-color two-photon (2c2p) excitation. For the first time femtosecond laser pulses are used to excite fluorescence by simultaneous absorption of two photons of different wavelengths.

1.2 History of microscopy

During the last century a variety of microscopic techniques has been established. Apart from the optical microscopy two other types of microscopes have to be mentioned: The scanning probe microscopes and the electron microscope. But even though these methods provide detailed information about the surface or thin slices of a sample with extremely high resolution, they are not suited for *in vivo* monitoring. The preparation of samples for these methods does not allow live imaging of biological samples. They require laborious preparation of biological samples which does not allow observing the undisturbed biological system in real time. Therefore, optical microscopy is still the method of choice for *in vivo* microscopy.

Classical optical light transmitting microscopy provides impressive images. Especially when modern contrast enhancing techniques like phase contrast or differential interference contrast (DIC) are used. However, one has to keep in mind that the obtained picture is a topographic

image of rather unspecific origin. The differences in brightness in the image originate from a mixture of light absorption and light scattering. When using phase contrast information about the phase shift of the transmitted light is added. In the case of DIC information about the optical density is added. Hence, the image contains an inseparable mixture of chemically rather unspecific information. This is contrasted by the demands of modern biology which focuses more and more on the molecular and therefore, chemical procedures inside biological systems.

Fluorescence microscopy can provide this desired chemical resolution. By choosing the appropriate excitation and emission wavelengths a selective monitoring of different fluorophores is possible. So, fluorescent biomolecules can be excited and the resulting autofluorescence can be monitored. In addition, a huge variety of fluorescent molecular tool has been developed. One can choose whether to selectively label specific parts of the sample or to monitor certain parameters inside an organism via specially designed fluorescence lifetime sensitive probes. These probes have been developed for almost every interesting cell parameter. The most modern fluorescent tool are genetically encoded fluorescent proteins which can be expressed at virtually every desired spot inside a living organism giving direct insight into its biochemistry.

1.3 Fluorescence Microscopy

Over the last four decades fluorescence microscopy has become an essential tool especially in bioscience, but also in technical applications like surface analysis. Fluorescence microscopy started with illumination and, hence, excitation using conventional light sources combined with filters. First fluorescence microscopes used a so called “wide field” illumination setup where the whole field of vision is illuminated at once using defocused light emerging from the microscopes objective. Fluorescence is collected by the same objective and can be monitored through a set of filters. This method is suitable for impenetrable surfaces or thin layers. However, for thick biological samples it yields highly blurred images. The reason for this is the lack of depth resolution. Fluorescence is excited not only in the focal plane but also above and below it. Since these out of focus fluorescence photons are also projected on the ocular or camera a blurred image is obtained.

Depth resolution in fluorescence microscopy was first provided by confocal microscopy.[1] A parallel laser beam is focused through the objective and scanned in a line-by-line mode over the sample. Again, the fluorescence is collected through the same objective. Because of the focused illumination, the depth resolution can be achieved due to a pinhole in front of the detector cutting off any fluorescence signal that does not originate from the focal plane of the objective. But still, using a one photon absorption for excitation following the Lambert-Beer's Law, excitation occurs along the complete path of the light through the sample and most of this excited fluorescence is discarded. Nevertheless, confocal microscopy represents a revolutionary new technique in the field of fluorescence microscopy since it allows for the first time to perform optical sectioning and hence, a complete three dimensional imaging of a fluorescent sample. Disadvantages are the relatively high and unnecessary photo stress in the out of focus area of the sample and the relative low quantum efficiency arising from the pinhole setup when high spatial resolutions are desire. Another inherent problem in both discussed fluorescence microscopy methods is the difficulty of separating the fluorescence signal from the excitation light in order to receive high contrast images.

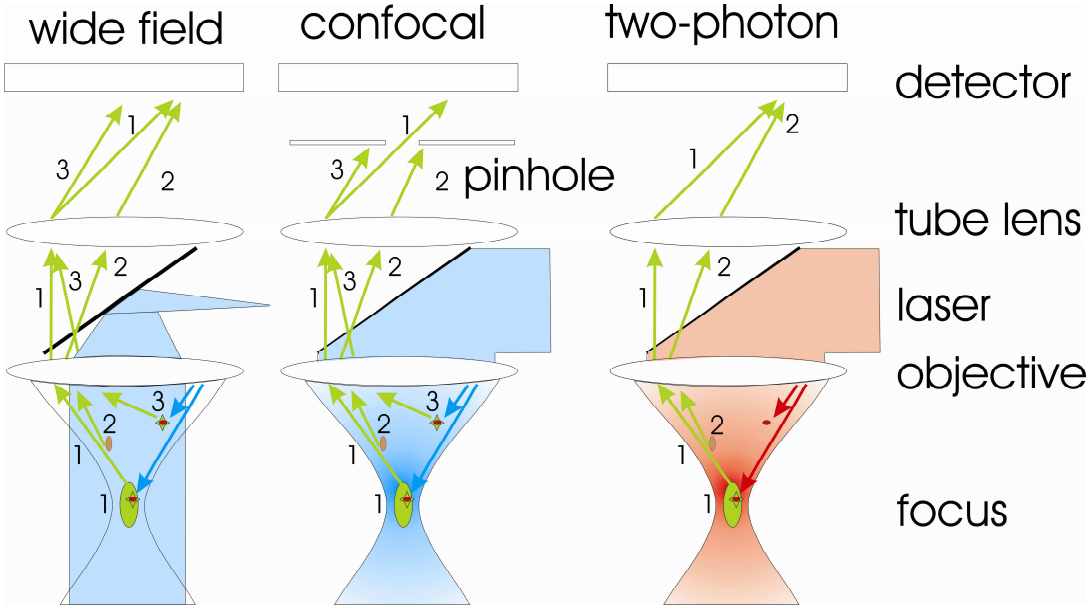

Figure 1.1: Comparison of the three different types of fluorescence microscopes. The numbers mark different events which can take place under the objective. 1 illustrates the excitation of a fluorophore in the focal volume. Fluorescence light from this point reaches the detector in all cases. In case 2 a fluorescence photon originating from the focus is scattered by the turbid sample. In wide filed microscopy this leads to a blurred image, in confocal microscopy the photon is lost at the pinhole, and in TPM the effect on the picture depends on the detection system: if a camera is used a blurred image will be obtained. Using a photo multiplier tube (PMT) or a photo diode the scattered photon will be assigned to its origin resulting in no blurring. Case three illustrates a molecule out of the focal plane. In wide field and confocal microscopy it will be excited and emit its fluorescence photon. In wide field this again leads to a blurred image. In confocal microscopy however, the photon is blocked by the pin hole. Only in TPM the out of focus molecule is not excited at all. This keeps the overall photo bleaching low as it is limited to the focal volume.

This is due to the relative small spectral Stokes shift between excitation and fluorescence spectrum of most fluorophores.

A second revolution in fluorescence microscopy was the invention of the two-photon laser scanning microscopy (TPLSM) in 1992.[2, 3] Using the double wavelength and a two-photon process for excitation provides numerous advantages. First of all, the long wave excitation, typically in the IR region, eases the separation of excitation and fluorescence light resulting in high contrast pictures. Secondly, it offers a higher penetration depth into biological samples due to much smaller absorption coefficients in the IR than in the visible region. However, the main advantage is that due to a quadratic dependence of the excitation probability on the excitation power the fluorescence is limited to the focal volume of the objective only. Hence, fluorescence is excited only where it is desired for detection. This keeps the photo damage done to the sample as low as possible. And, of course, this leads to an intrinsic three dimensional resolution of this method making the complicated and signal attenuating implementation of a pinhole setup obsolete. These advantages have helped TPLSM to become an indispensable tool in biosciences. TPLSM is the superior fluorescence microscopy especially when it comes to *in vivo* imaging where low photo damage and high penetration depth is desired.

These three fluorescence microscope techniques, wide field, confocal and TPM have developed to reliable work horses which can be found in many biological or medical laboratories. Today, research in the field of fluorescence microscopy mainly focuses on improving the spatial resolution of these techniques beyond the diffraction limit defined by Abbe's law. For wide field microscopy best results can be achieved using structured illumination techniques allowing resolutions close to 10 nanometers[4, 5] For the confocal laser scanning technique most impressive resolutions beyond the diffraction limit can be achieved using the stimulated emission depletion (STED) technique,[6, 7] where the focal excitation volume is decreased after excitation by stimulated emission and therefore, depletion of the excited state with a second laser possessing a specially shaped focal volume. In both techniques the resolution is increased by adding additional information via non linear effects.

Other approaches suitable for all three fluorescence techniques are the use of photo switchable fluoresophores (PALMIRA = photoactivation localization microscopy with independently running acquisition) as well as statistic methods (STORM = stochastic optical

reconstruction microscopy) employing the spatial distribution of photons emitted from single molecules.[8, 9] Fitting a Gaussian function to the data obtained from samples with fluorophores in very low concentration determines their position down to few nanometers.

However, there are still other problems to be addressed apart from improving the spatial resolution. TPLSM for example suffers from extremely small tow-photon absorption cross sections. This requires high excitation to obtain reasonable absorption rates and fluorescence signals. These powers can only be provided by the lasers with short pulses. The shorter the pulse duration, the smaller the introduced amount of energy is. Only this way it can be kept at a level that can be tolerated by the sample under investigation. Today, the ideal light source for a TPLSM is the Ti:Sa femtosecond laser. With pulse lengths of a few to hundreds of femtoseconds and repetition rates of typically around 80 MHz it combines low energies per pulse of typically few nJ with sufficient excitation rates.

Although the Ti:Sa is known for its extraordinary broad continuous laser spectrum it is still limited to a spectral windows of about 700 nm to 1100 nm corresponding to effective two-photon excitation wavelengths from 350 nm to 550 nm. The definition of this spectral window of a two-photon absorption sticks to the paradigm that the two photons involved in the excitation process originate from the same laser beam and therefore, are of the same color.

The aim of this thesis is to investigate the extension of two-photon laser scanning microscopy (TPLSM) to two-color two-photon laser scanning microscopy (2c2pLSM) meaning that two different photons are absorbed simultaneously for excitation. In addition to the new possibilities arising from the extended spectral window most of the advantages of TPLSM do also apply for 2c2pLSM. This is mainly due to the fact that the absorption rate is proportional to the product of the intensities of each of the two colors. This leads to an intrinsic three dimensional resolution like in TPLSM as it limits the excitation to the volume where both beams overlap spatially and temporarily. Additionally, using an excess power at 800 nm combined with low 400 nm power levels to provide sufficient excitation rates leads to high penetration depths and low photo bleaching. Hence, the main excitation power is transported via the 800 nm beam which can easily penetrate the sample.

The phenomenon of 2c2p absorption has been studied previously. In 1964 McClain et al. performed fundamental studies about the absorption process using a combination of ruby laser and a flash lamp.[10] The absorbing medium was a pure liquid phase. Later, in 1996 Lakowicz et. al. performed first 2c2p fluorescence experiments.[11] In his work picoseconds dye laser

and dyes in solution are used. He also suggests extending these experiments to a microscopic method. But no results of such an attempt have been published to date.

2 Overview over the presented work

In this thesis three publications about experiments toward 2c2pLSM are presented. The first publication deals with fundamental fluorescence experiments where the possibility of 2c2p excitation of fluorophores using femtosecond laser pulses is demonstrated. Therefore, three suitable dyes are characterized. The use of femtosecond pulses is inevitable to make 2c2p microscopy effective and applicable. Therefore, a classical perpendicular fluorescence setup is used for these experiments. Using the fundamental 800 nm beam of a Ti:Sa together with its frequency doubled 400 nm beam results in an energetic one-photon absorption equivalent of 266 nm. One of the dyes is tryptophan, the amino acid which is responsible for the majority of protein fluorescence. The possibility of effectively exciting it is the key experiment leading to later applications of this technique to label free protein fluorescence studies.

Consequently, the second part of this thesis deals with an application of intrinsic protein fluorescence resulting from a 2c2p excitation. The proteolytic digestion of bovine serum albumin (BSA) by an enzyme is monitored by means of fluorescence lifetime. The fluorescence lifetime of tryptophan is very sensitive to its environment and especially to its binding conformations influencing the amount of quenching and, hence, the lifetime of the excited state. During the digestion process the fluorescence lifetime decreases while the protein is successively cleaved into smaller fragments. Hence, tryptophan acts as a natural built in probe for monitoring the digestion of a protein.

The sensitivity of this 2c2p fluorescence method was then increased using another experimental setup. In this microscope setup both colors are confocally focused through a microscope objective which also collects the fluorescence for detection. Apart from the inherent possibility of using this setup to perform laser scanning microscopy the high numeric aperture objective used provides a much higher efficiency in terms of excitation as well as for fluorescence detection. Not till then, it was possible to monitor the digestion of human serum albumin (HAS) which contains only one single tryptophan per protein molecule. The third publication presented in this thesis presents 2c2pLSM images of MIN-6 cells. Intrinsic protein fluorescence is excited inside the living cells using 2c2p excitation. Fluorescence in collected

using a time correlated single photon counting (TCSPC) system with an avalanche photodiode (APD) as detector. Allowing good temporal resolution, these measurements revealed differences in fluorescence lifetime of the autofluorescence of cells in the UV regime. Additionally, application of 2c2pLSM was demonstrated on monitoring the binding of biotin to avidin via the fluorescence lifetime of the avidin fluorescence.

3 Theory

3.1 Excitation of Fluorescence

Fluorescence is a luminous phenomenon following electronic excitation. The energetic processes after electronic excitation of a molecule will be explained in the fluorescence lifetime section. The classical way of exciting the sample is using light at the wavelength matching the energy gap between electronic ground state S_0 and the first excited state S_1. In the following this is referred to as one photon excitation. In addition, there are also different ways of exciting the sample using nonlinear optical effects.

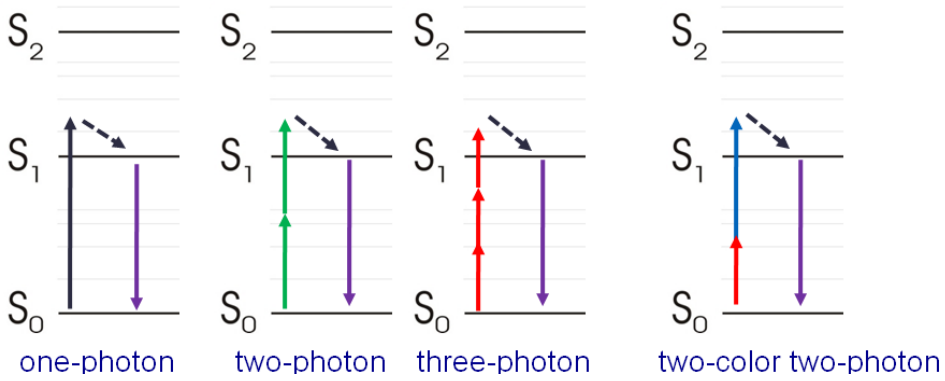

Figure 3.1: Jablonski Diagram illustrating the different ways of excitation of fluorescence.

Two-photon excitation means that light of double the wavelength is used while three-photon excitation means the use of light of triple the wavelength of an equivalent one-photon absorption. The photons needed for providing the excitation energy are absorbed simultaneously. Two-color two-photon absorption means that two arbitrarily chosen wavelengths can be used for excitation as long as there sum of energy matches the excitation energy. Again, the two photons responsible for the excitation have to coincide to be absorbed simultaneously. This is what makes the nonlinear optical effects to be far less probable to

happen under low light conditions. A huge photon flux is usually needed to provide sufficient absorption rates.

For an one-photon absorption this rate is proportional to the light intensity I used for excitation. The proportionality factor is σ which usually has values in the range of 10^{-15}cm². With N meaning the number of molecules in the ground state the one photon absorption rate can be described by

$$\frac{dN}{dt} = -\sigma \cdot I \cdot N. \qquad (1)$$

In the case of a one color two-photon absorption the absorption rate depends on the square of the excitation intensity.

$$\frac{dN}{dt} = -\delta \cdot I^2 \cdot N \qquad (2)$$

with δ as two-photon absorption cross section lying in the region of about 10^{50} cm^4/s. Hence, high light intensities are required to provide a sufficient excitation rate. For microscopy it is not possible to provide this excitation power by continuous wave lasers. Lasers with several kilowatts of excitation power are needed. The application of energy to the sample by such a laser is too high to be tolerated by any sample. The dilemma of the need for high excitation powers and the relatively limited tolerance of the samples for application of energy is solved by the use of femtosecond pulse lasers. A typical femtosecond laser running at 80 MHz and a power of 1 W emits 80 million laser pulses with a pulse duration of 200 fs. This means that the laser emits a power of 1 J over a time of 1 one second. Divided by 80 millions this yields an energy of 12.5 nJ per pulse. Since this small energy portion is emitted during the ultra short laser pulse of only 200 fs this result in an impressive power of 62,5 kW during the pulse. Excitation efficiency increases with shorter pulses. The shorter the pulse, the higher the maximum power during the pulse at the sample laser output. For two-photon microscopy applications femtosecond laser powers of typically few milliwatts are sufficient.

For the above description of the absorption rate both photons have the same color. Two-color two-photon (2c2p) excitation uses two different photons where the energies of the two photons have to sum up. Now the excitation rate is dependent on the product of the intensities.

$$\frac{dN}{dt} = -\delta \cdot I_{\lambda 1} I_{\lambda 2} \cdot N \qquad (3)$$

This offers the possibility of using different intensities at both wavelengths. Hence, the excitation can be adjusted to the requirements of the experiment. For deep tissue imaging for example it is favorable to use a higher power at the longer wavelength which is less absorbed and scattered. The shorter wavelength which is potentially more absorbed and can be used with lower power to prevent photo damage.

3.2 Fluorescence Imaging

In fluorescence microscopy a vast variety of different sources of fluorescence can be used for imaging. Biological samples can be stained using specially designed dyes. Different dyes label different parts of cells.[12] Other dyes are designed as fluorescent probes for parameters like Ca^{2+} or Mg^{2+} concentration, or pH.[13-15] These dyes indicate different concentration via changes in the absorption and / or emission spectrum. Hence, ratiometric measurements using two excitation or emission wavelengths can reveal changes in the relevant parameter. Staining biomolecules like antibodies offers an almost endless arsenal of tailored fluorescent probes that can be prepared.

Today, the most sophisticated but also most elaborate method is to use genetically encodes fluorescent proteins like green fluorescent protein (GFP) and its derivatives.[16] It is possible to fuse GFP to every cloneable protein by combining the DNA of the protein and the GFP.[17] Different techniques have been developed to introduce cloned DNA in the organism of the sample. The fluorescent protein is then expressed via the protein synthesis mechanisms of the organism.

Although, the use of fluorescent dyes is a tool box with enormous potential it has disadvantages. First of all it is not the undisturbed biological specimen which is under observation. Even though only low concentration are required for sufficient staining it is still the introduction of a foreign substance into the biochemical system of the sample potentially can altering its behavior. Secondly, staining means one or more steps of preparation and therefore, stress applied to the sample. Often auxiliary substances like solvents or detergents are used to allow the dye entering the cell which of course can lead to an additional alteration of the biological sample.

Genetically encoded fluorescent proteins like the GFP moiety with its molecular weight of 27 kDa are of considerable size. This can potentially alter the behavior of the protein. Furthermore, the concentration of the expressed protein GFP complex will be adjusted according to the necessities of the fluorescence imaging system. These concentrations will in many cases exceed those of the endogenous protein concentration.

For monitoring the undisturbed sample it can therefore be desired to use naturally available fluorophores inside the sample. Many bio-molecules fluoresce. Important intrinsic fluorophores are for example the structure proteins ceratine, kollagene and elastine or the pigment melanine but also nicotinamide adenine dinucleotide phosphate (NAD(P)H) and flavin adenine dinucleotide (FAD) which are part of the cell metabolism.[18]

These fluorophores have their absorption and emission spectrum in the visible range. Hence, their fluorescence is relatively often used for fluorescence imaging.

The fluorescence of the fluorescent amino acids tryptophan and tyrosine can also be used for fluorescence imaging. Implemented into the structure of many proteins they act as a natural fluorescence tag. Both amino acids fluoresce, but the quantum yield and absorption cross section of tryptophan are higher. Excited tyrosine can also transfer its energy to tryptophan via a resonant mechanism.[19] Thus, it is mainly the tryptophan fluorescence that is monitored when studying protein fluorescence. Besides the topographic information about the distribution of these amino acids inside the cell a detailed analysis does often reveal even more information about the protein. This additional information can be obtained from spectrally resolved measurements as well as from time resolved anisotropy of fluorescence lifetime measurements.[20-23] The challenge for fluorescence microscopy is that the absorption spectrum of tryptophan has a maximum at 280 nm, i.e. UV. This wavelength is problematic for several reasons. First of all UV light possesses a high photo toxicity for biological tissue. Secondly it is highly scattered in turbid media. And moreover it requires the use of special optics since the conventionally used objectives or lenses in fluorescence microscopes are not transparent for wavelengths shorter than 300 nm.

These problems can be solved by multi-photon excitation. Irradiating light at the doubled wavelength (TPM) is less toxic for the sample. Due to the quadratic dependence of the excitation rate on the excitation power the excitation is limited to the focal volume only. This reduces the overall photo bleaching and therefore, the photo toxcicity. However, nowadays femtosecond laser pulses at 560 nm with sufficient power and repetition rate are not

accessible. Furthermore, irradiation of 560 nm light at intensity sufficient for two-photon excitation is problematic because of the high absorption of biological samples in the visible range. 2c2p offers the possibility of applying the main intensity required for excitation via the less harmful 800 nm beam while only low intensities of the potentially harmful 400 nm light are needed.

3.3 Fluorescence lifetime

Once a molecule is excited, it has different way to dissipate this energy. In a first step the molecules will undergo a vibrational relaxation called internal conversion to return to the vibrational ground state of the first excited electronic state. This usually takes place on a time scale of picoseconds. Once in the vibrational ground state there are numerous options of what happens next to the energy of the molecule. It can further relax in a vibrational way k(des). This relaxation is highly dependent on the surrounding of the fluorophore. Since it is a radiationless process the energy has to be transferred to its neighbor molecules. Another possibility is that inter system crossing occurs r(ISC) meaning a spin forbidden transition into one of the triplet states of the molecule. From there again vibrational relaxation and /or emission of radiation can occur. This emission takes typically place on a time scale of millisecond to seconds because of the spin forbidden transition to the singlet groundstate of the molecule. Other pathway of the excitation energy lead to charge transfer r(CT) or even reaction r(rktn). For fluorescence microscopy it is of course the occurrence of fluorescence which is the most desired option. The fluorescence rate is dependent on its fluorescence rate constant k(fl) and on the population of the first excited electronic state. If k(fl) is the only process leading to a depopulation of S_1 the k(fl) simply reflects the natural fluorescence lifetime $\tau_{0.}$

$$\tau_0 = \frac{1}{k(fl)} \qquad (4)$$

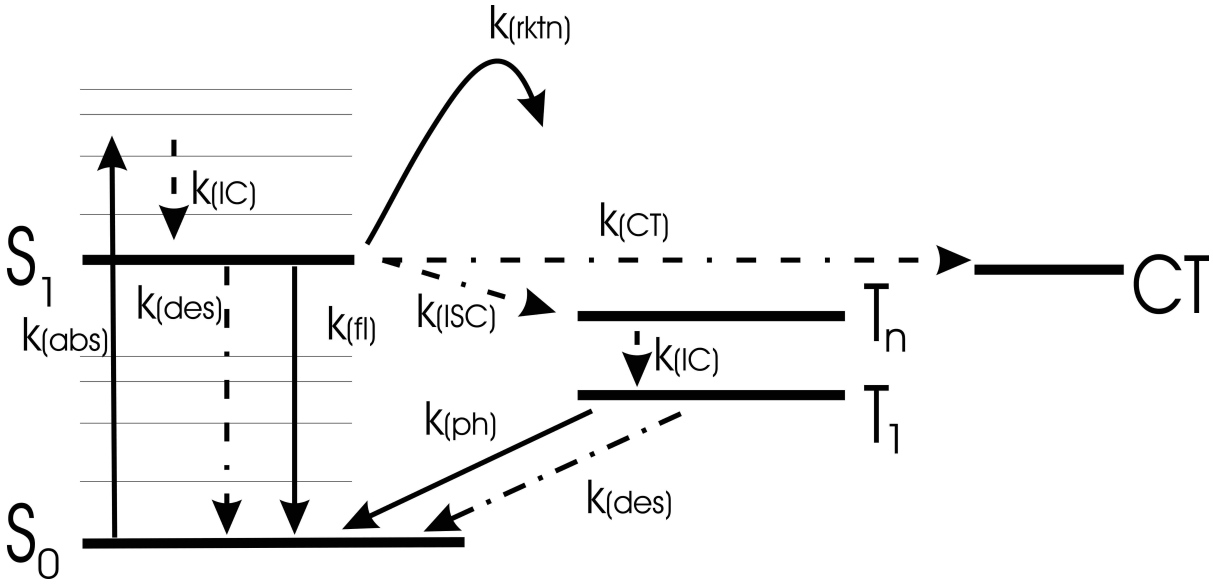

Figure 3.2: Jablonski Diagram illustrating the different possibilities of energy dissipation out of the excited state. The different k represent the rate constants for the different pathways. IC means internal conversion, rktn reaction, CT charge transfer, des desactivation without radiation, abs absorption, fl fluorescence, ISC intersystem crossing, ph phosphorescence and fl stands for fluorescence.

In general, the observed rate of fluorescence is also dependent on the rates of competing processes leading to a depopulation of S_1. Hence for quantification of fluorescence a useful measure is rather the fluorescence quantum yield Φ_F than the rate fluorescence constant k(fl). Fluorescence quantum yield is defined as the ratio of the rates of emitted (r_f) to absorbed (r_a) photons. Expressed in rate constants it is the ratio of the fluorescence rate constant to the sum over all rate constants referring to processes leading to depopulation of S_1.

$$\Phi_F = \frac{k(fl)}{\sum k(relax)} = \frac{k(fl)}{k(fl)+k(des)+k(rktn)+k(CT)+k(ISC)} \qquad (5)$$

Since the competing processes also depopulate S_1 they consequently lead to an increased speed of depopulation. This shortens the time a fluorophore is able to emit fluorescence photons. Hence, the fluorescence lifetime is reduced when the fluorescence quantum yield is reduced.

$$\tau = \frac{\Phi_F}{k(fl)} = \frac{1}{\sum k(relax)} \qquad (6)$$

This is the basis for fluorescence lifetime measurements. Changes in fluorescene lifetime correspond to changes in the rates of competing relaxation processes and, therefore, measure changes in the environment of the fluorophore. What exactly is measured via a change in fluorescence lifetime depends on the design on the fluorophore. There are specially designed fluorophores whose fluorescence lifetime is dependent on a specific parameter while it in first

approximation independent on other parameters. With these fluorophores it is possible to measure e.g. concentrations of ions and oxygen, viscosity, temperature or the refractive index.[24-26]

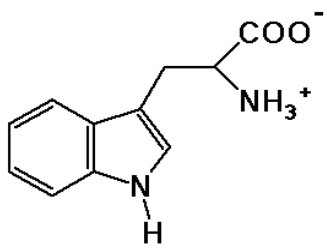

Figure 3.3: Tryptophan

A more complicated field of fluorescence lifetime measurements is the interpretation of fluorescence lifetimes of naturally occurring fluorophores e.g. NAD(P)H, flavine, elastine, ceratine. One especially complicated case is the amino acid tryptophan. Numerous fluorescence lifetime studies of tryptophan in different environments have been carried out.[20, 27-29] But to date, it is still impossible to precisely predict a fluorescence lifetime value for a typtophan in a specific environment. Its lifetime changes from about 1.5 ns when present in form of a tripeptide in solution to about 6 ns in proteins.[20, 27] Almost every value in between can be found depending on the position of tryptophan inside a protein. The possibilities for tryptophan to dissipate its absorbed energy inside a protein other than via fluorescence seem to be manifold. There are good indications that the binding angles of the bonds attaching the amino-acid group to the aromatic rings have a great impact on the fluorescence lifetime. This influence is explained by different interactions between the π system of the carboxylate and the mesomeric system resulting in different probabilities for charge transfer.[23] Other influences are the neighborhood of other aromatic amino acids.

4 Experimental

There will be a brief description of the experimental setup in each of the following chapters. However, more detailed information is given here. The first part describes an experimental setup where the two laser beams needed for 2c2p excitation are confocally focused into the sample vial an achromatic lens and where the fluorescence is detected perpendicular to the excitation axis. The second part deals with the extension of this setup to a 2c2pLSM microscope.

4.1 Perpendicular 2c2p fluorescence setup

An experimental setup for studying 2c2p excitation of fluorescence with femtosecond laser pulses is built using the fundamental and frequency doubled of a Ti:Sa femtosecond laser. Frequency doubling is achieved focusing the 800 nm beam into a β-bariumborate crystal (BBO). The frequency doubling efficiency is about 7 %. The polarization of the occurring frequency doubled light is perpendicular to the fundamental wave focused into the crystal. To ensure simultaneous arrival of the 800 nm and 400 nm pulse in spite of optical dispersion effects, both colors are separated using a dichroic mirror (DC_1 in figure 4.1). Therefore, a delay line in form of two perpendicular mirrors mounted on a motorized linear stage is implemented in the optical path of the 800 nm light. This delay line has to be very precisely because light travels only about 60 µm during the laser pulse duration of 200 fs. After this delay line the two colors are reunified with a second dichroic mirror and focused by an achromatic lens into the sample. It is crucial for the experiment that the spatial position of the 800 nm beam is not influenced by movement of the linear stage. In other words the spatial overlap must be unaffected from any adjustments to the temporal overlap.

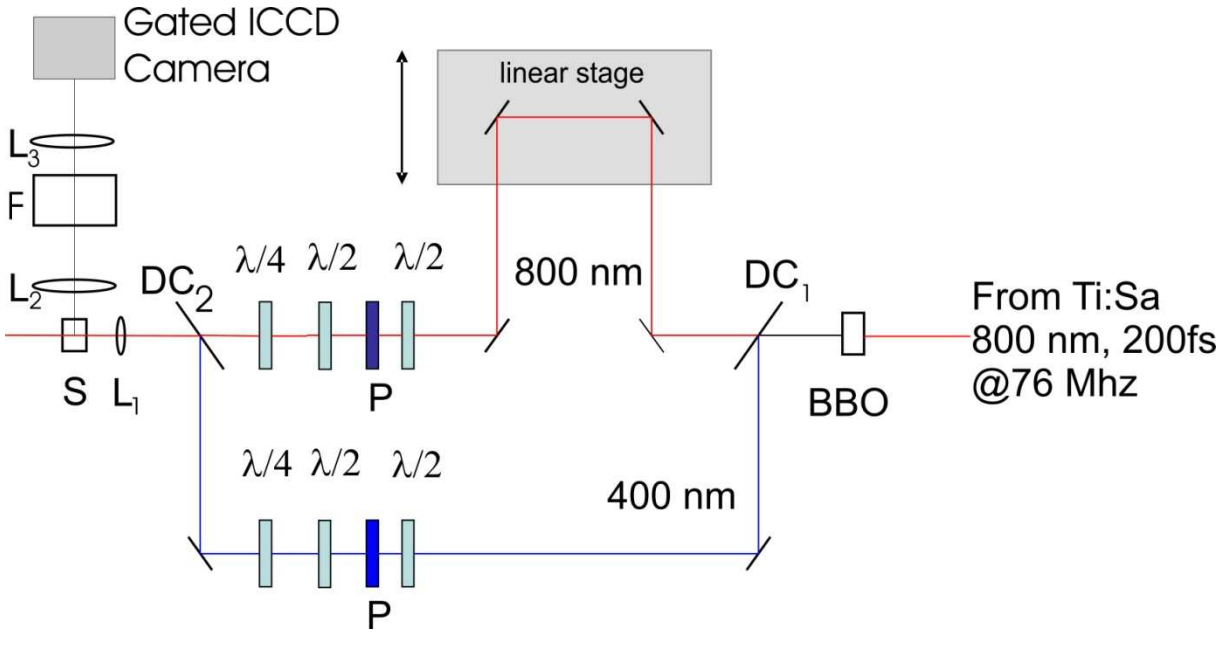

Figure 4.1: Perpendicular fluorescence setup for 2c2p fluorescence experiments

For first adjustment of spatial and temporal overlap a pinhole and a wave mixing crystal are used. Both of which can be mounted into the same position where a cuvette can be mounted later. First of all, both laser beams are adjusted to maximal transmission through the pinhole to ensure spatial overlap (figure 4.2 A).

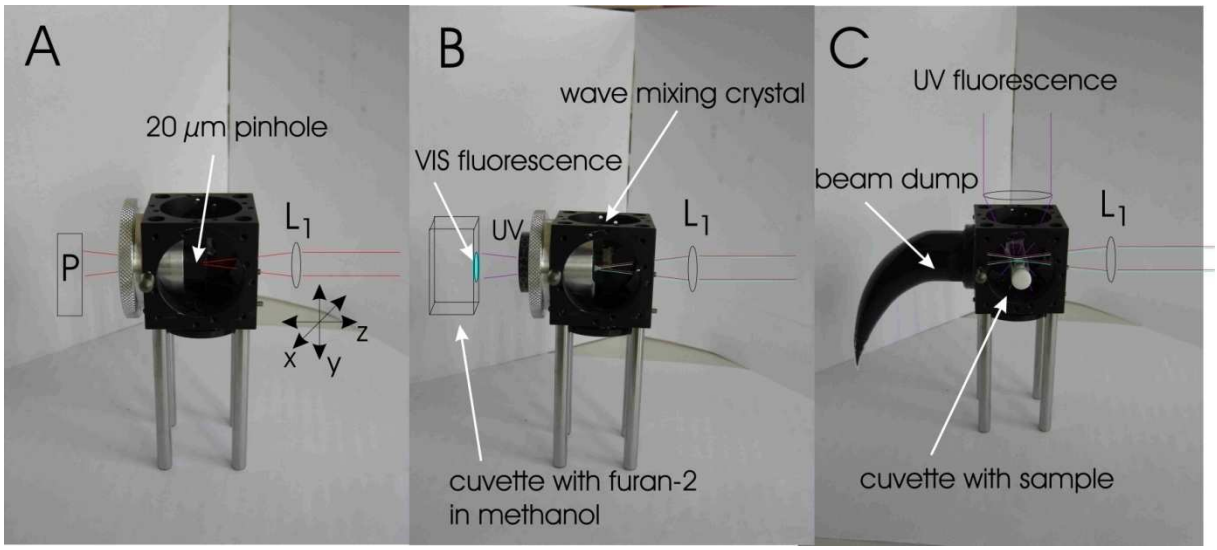

Figure 4.2: setup for adjustment of spatial and temporal overlap. A: Spatial overlap. The transmission through the pinhole is measured with a power meter P. After a coarse adjustment of the red beam to the pinhole Power is maximized by 3D adjustment of the achromatic lens L_1. Transmission power of the blue beam is adjusted by mirrors only. B: Temporal overlap. The pinhole is replaced by a wave mixing crystal. Temporal overlap is reported by occurrence of UV Light (266 nm) after the crystal, which is visualized via fluorescence of Furan-2 in methanol. C: 2c2p setup. The crystal is replaced by a cuvette containing the sample. UV fluorescence is gathered by a lens on top and lead to the detector. The excitation beams end in a beam dump (Wood's horn).

The red beam is coarsely adjusted to the center of the pinhole without the lens L_1 in position. Now the lens is introduced into the light path. To find the optimal position of the lens, transmission power through the pinhole, which is measured using a power meter after the pinhole, is maximized by 3D adjustment to the lens using linear stages. Once the optimal position of the achromatic lens is found, the blue laser beam is adjusted by optimizing its pinhole transmission via the position of the dichroic mirror DC_2. In advance, it is crucial that the blue and red laser beam leave this dichroic mirror at exactly the same spot to ensure parallelism.

Now the pinhole is substituted by the wave mixing crystal in the same position to find the temporal overlap (figure 4.2 B). It is worth to note that a 200 fs pulse corresponds to a difference in optical path length of only 60 µm. Spatial overlap of the two beams and correct angle of the wave mixing crystal provided, temporal overlap is indicated by emission of a 266 nm beam on the same optical axis of the two incident beams. For purpose of visualization of the 266 nm light both incident laser beams are blocked using a 270 nm interference filter right after the wave mixing crystal. A quartz cuvette filled with a solution of 2-(4-biphenylyl)-6-phenylbenzoxazotetrasulfonicacid potassium salt (furan-2) in methanol is positioned behind this filter. Now the 266 nm light can be detected by eye via the blue fluorescence of Furan-2.

Having spatial and temporal overlap successfully adjusted, the sample cuvette is mounted instead of the wave mixing crystal (figure 4.2 C). It should be noted that minor adjustments to the delay line are necessary for solvents with different refraction indices to achieve optimal 2c2p excitation. 2c2p fluorescence is collected via a quarz lens on top and filtered with a 350 / 40 nm interference filter combined with two notch filters (Semrock^{TM}). The notch filters posses a central wavelength of 808 nm and 405 nm, respectively. Both filters are tilted approximately 12 ° to have their central reflection wavelength match the requirements of the experiment.

4.1.1 Detection system

Finally, the fluorescence is projected onto a time gated CCD camera system (PicoStar, LaVision, Göttingen). This camera system consists of a gateable multi channel plate (MCP) and a conventional cooled CCD camera. The MCP consists of a photo cathode where a bias can be applied. A photon hitting the photo cathode will release an electron from the cathode that will then follow the bias into small metal coated channels. While flying through these very thin (few microns) channels the electron will very likely hit the wall. This collision will release additional electrons. Hence, instead of a single photo electron a whole cloud of electrons will leave the channel of the MCP. These electrons then hit a phosphorus screen where they excite fluorescence. This fluorescence is then detected by a CCD camera. Because of the high number and small dimensions of the channels the spatial distribution and therefore the image information is generally retained.

The photocathode of the MCP can be gated with an accuracy of 11 ps and an adjustable gate length of 200 ps to 1 ns. This means that only for this short period the bias is applied and pulls the photo electrons off the photo cathode into the amplification channels of the MCP. Only photons arriving at the photo cathode during this time period are amplified and registered by the CCD camera. For time resolved measurements the gate can be temporally shifted by a delay generator in steps as small as 25 ps with respect to the laser pulse.

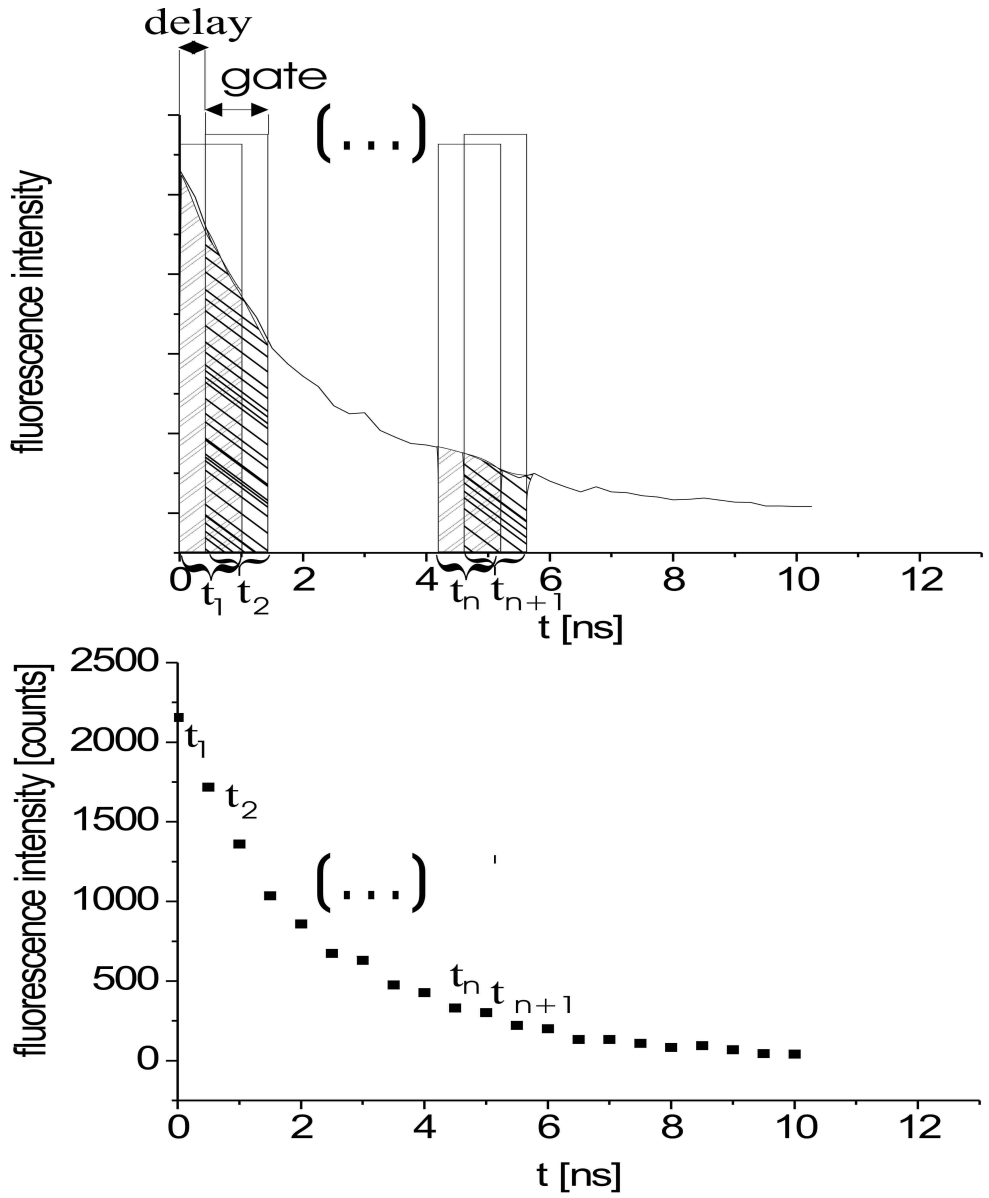

Figure 4.3: Time gated detection methode. To the photo cathode of the time gated camera system voltage is applied only for a short period of time after each laser pulse. This time period is called "gate". The width of this gate can be adjusted from 0.2 ns to 1 ns. By adjusting the relative delay of this gate with respect to the laser pulse the fluorescence lifetime curve can be measured.

Figure 1.7 illustrates such a time resolved measurement. At time t_1 the delay is set to 0 ps relative to the laser pulse. The gate width is set to 1 ns. Now all fluorescence photons arriving during the first nanosecond after each laser pulse will be counted for a preset number of laser pulses. The number of laser pulses is determined by the acquisition time which is typically in the range of ms to seconds. For a single exponential decay $e^{-t/\tau}$ the gated camera observes the signal S:

$$S = \int_t^{t_g} e^{\frac{-t}{\tau}} dt \qquad (7)$$

where the gate opens at time t and closes at t+ t_g. Integration yields

$$S = \tau \cdot e^{\frac{-t}{\tau}} \cdot (1 - e^{\frac{-t_g}{\tau}}). \qquad (8)$$

The expression in brackets is constant and thus, the observed a signal is proportional to $e^{-t/\tau}$. The gate is then shifted by the delay generator with high precision to measure the step-by-step fluorescence decay curve. For each step all photons are counted during the time period of the gate summed over the same number of laser pulses. It is the high precision of the delay generator combined with the uniformity of the gate enabling the system to achieve high temporal resolution. The jitter of the delay is only about 10 ps. This corresponds well with the best achieved temporal resolution.

4.1.2 Adjustment of excitation power and polarization

For power adjustment each optical path of the two laser beams has a combination of λ/2 wave plate and a thin layer polarizer (see figure 4.1). The thin layer polarizer is adjusted with respect to the table surface to let s polarized light pass. Now the power level can be adjusted by turning the λ/2 wave plate. Additionally, a combination of an additional λ/2 wave plate and a λ/4 wave plate is implemented in each path in order to provide all possible polarization states without changing the optical delay by introducing polarization optics. The s polarization of the laser light after the thin layer polarizer can be retained by adjusting both retard plates at 0°. Now the light passes parallel to one of the main axis of each birefringent plate leaving the polarization unaltered. When p polarized light is desired the λ/2 wave plate is rotated by 45 °. This results in a rotation of the polarization of 90 °, hence, in p polarization (figure 4.4).

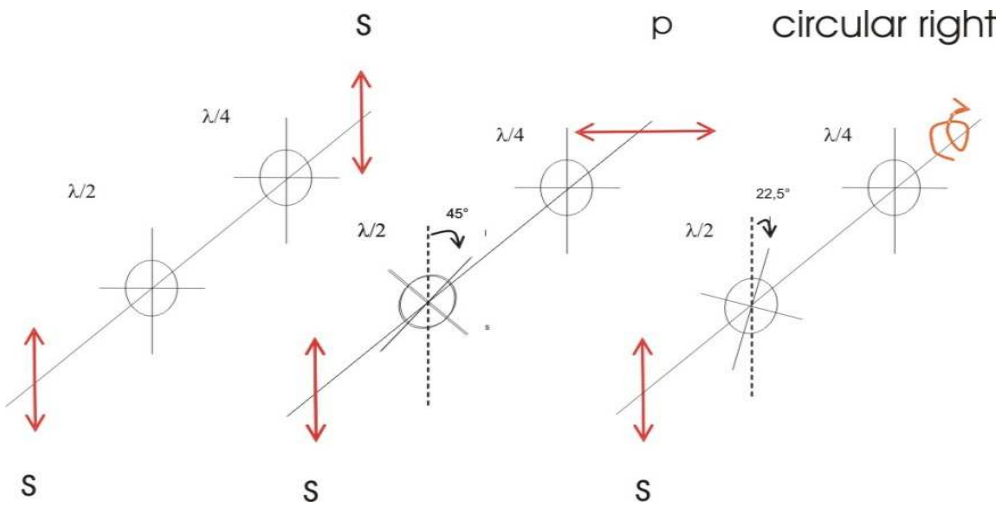

Figure 4.4: Adjustment of polarization. The propagation direction of the s polarized light is from front to back. Left: Both retard plates are adjusted in a way that the polarized laser light passes parallel to one of their main axis. The polarization of the light is not affected. Middle: Rotation of the λ/2 plate by 45 ° results in a rotation of the polarization of the light by 90 °. Now the p polarized light passes the λ/4 wave plate parallel to its other main axis and remains unaltered. Right: Rotation of the λ/2 plate by 22.5 ° results in a rotation of the light polarization of by 45 °. Passing the λ/4 wave plate at this angle results in circular polarized light.

The λ/4 wave plate is now passed by the laser light parallel to its other main axis leaving the p polarization unaltered. Circular polarization can be achieved by rotation the λ/2 wave plate by 22.5 °. This results in a rotation of the initial s polarization of the light by 45 °. Passing the λ/4 wave plate at this angle results in circular polarized light. The sense of rotation depends on whether the λ/2 wave plate is rotated by +22.5 ° or -22.5 °.

To verify the sense of rotation and to have a measure for the degree of polarization of the circular polarized light a combination of a Fresnel Rhomb and a polarizer is used (figure 4.5).

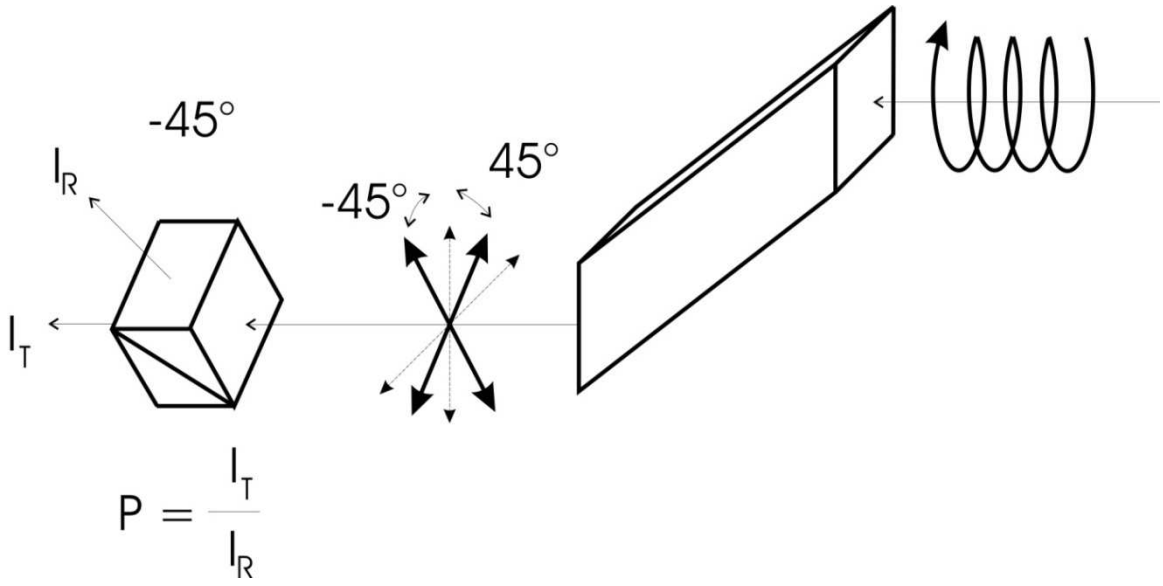

Figure 4.5: Measuring the degree of polarisation of circular light. Circular light entering a Fresnel rhomb is turned into linear polarized light that leaves the Fresnel rhomb at a 45 ° angle. Circular light with an opposite sense of rotation results in linear polarized light leaving the rhomb at an -45 ° angle. The degree of polarization can be determined by measuring the intensities of the transmitted (I_T) and reflected (I_R) light leaving the polarizer.

A Fresnel Rhomb turns circular polarized light into linear polarized light. The polarization is oriented at a 45 ° angle in respect to the Fresnel Rhomb. If the rotation is + or – 45° depends on the sense of rotation of the circular polarized light and on the orientation of the rhomb and has to be determined for each setup. The main advantage of a Fresnel rhomb over a λ/4 wave plate is that its polarization behavior is almost independent on the wavelength. Hence, the presented setup can be used to measure the degree of polarization of both the 800 nm and the 400 nm beam with the same setup at a position right in front of the sample.

If perfectly circular polarized light enters the Fresnel rhomb the light will leave it with exactly 45 ° or -45 ° depending on the sense of rotation. Elliptic polarized light results in a linear polarization after the Fresnel Rhomb at an angle other than 45 °. Therefore, the degree of polarization of the circular polarized light corresponds to the degree of polarization that can be measured using a polarizer at exactly 45 °.

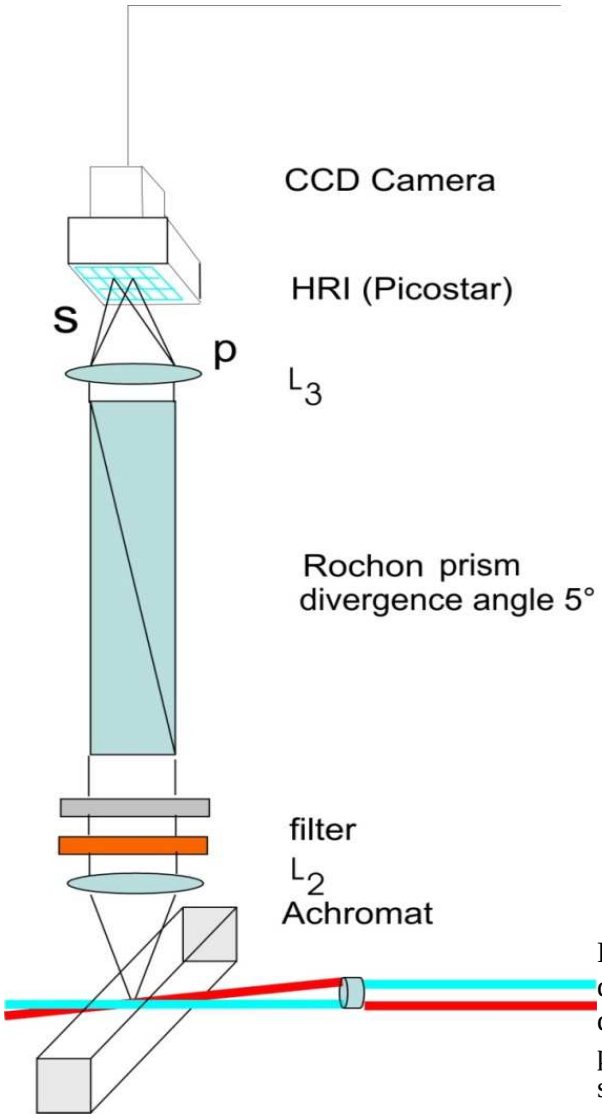

Figure 4.6: Polarization and time resolved detection. A Rochon prism with 5° divergence angle projects the two polarizations on different areas on the camera system.

4.2 Fluorescence anisotropy

Time dependent anisotropy measurements can be performed installing a Rochon Prism into the parallel part (between L_2 and L_3) of the fluorescence detection path. A prism with 5° separation angle is used. The separated polarizations are then projecting through lens L_3 onto the time gated camera system. Now the fluorescence intensity can be read out for each polarization separately (figure 4.6).

4.3 2c2p microscope

Next step of development of the experimental setup is the realization of a 2c2p laser scanning microscope. Two different setups will be discussed. One based upon beam scanning and camera detection. The other based on sample scanning and non-descanned detection using an avalanche photo diode.

4.3.1 Beam scanning setup with camera

The perpendicular fluorescence setup including the lens behind the second dichroic mirror (see figure 4.1) is removed and a fluorescence microscope is installed instead.

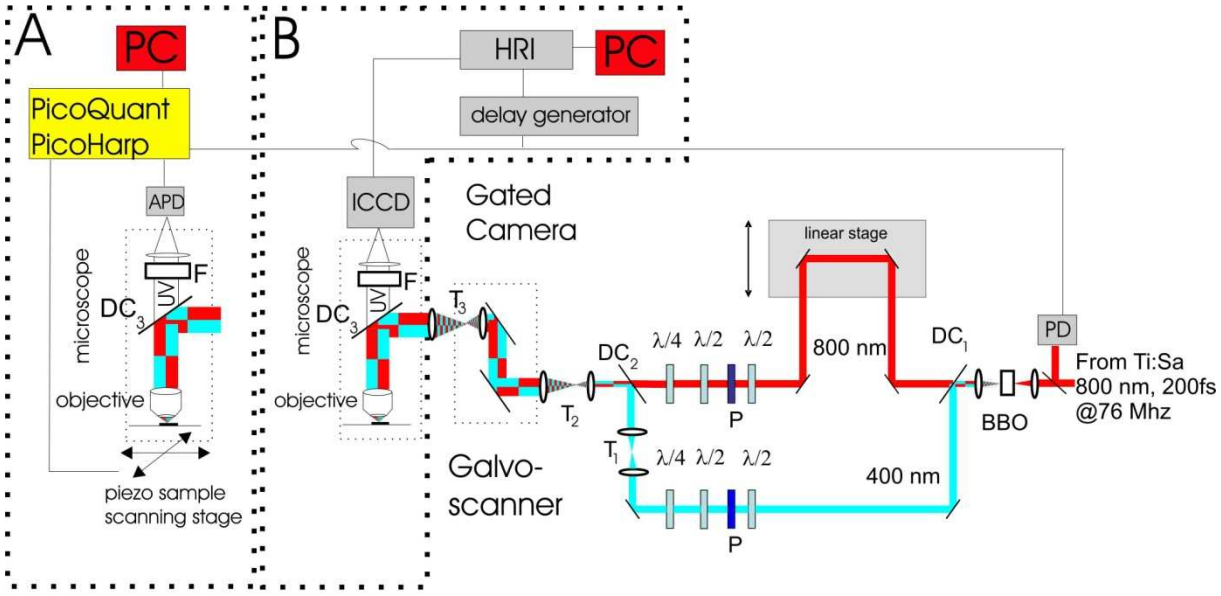

Figure 4.7: 2c2pLSM setup. A: Sample scanning setup with an avalanche photo diode (APD) and TCSPC detection. B: beam scanning setup using a galvo scanner and a time gated camera system for detection.

To ensure optimal focusing both laser beams are expanded in two steps before reflected into the microscope objective using telescopes. To account for the chromatic aberration the path of the blue light contains another telescope that can be misadjusted. After the first telescope a Galvo scanner (GSI Group GmbH, Munich) is placed. The center of the galvo driven mirrors is then projected via a second telescope onto the back aperture of the microscope objective for optimal scanning process via a dichroic mirror. A Zeiss Achroplan 40x 1,3 NA and a HCX PL Apo 100x 1,4 NA oil immersion fluorescence objective are used. The fluorescence gathered

by the objective passes the dichroic mirror, is filtered by the same set of filters which was installed in the perpendicular setup and is again focused by a quartz lense onto the gated camera system.

The spatial resolution of this setup is limited. A general problem is the blur introduced by the multichannel plate of the intensifier of the camera system. Even single photons hiting the photo cathode result in signals on multiple pixels of the CCD camera. This problem can be reduced by increased magnification between the microscope and the MCP intensifier to ensure that the resolution of the image is transferred lossless on the CCD chip of the camera.

Without magnification the image is blurred and the resolution provided by the objective cannot be used.

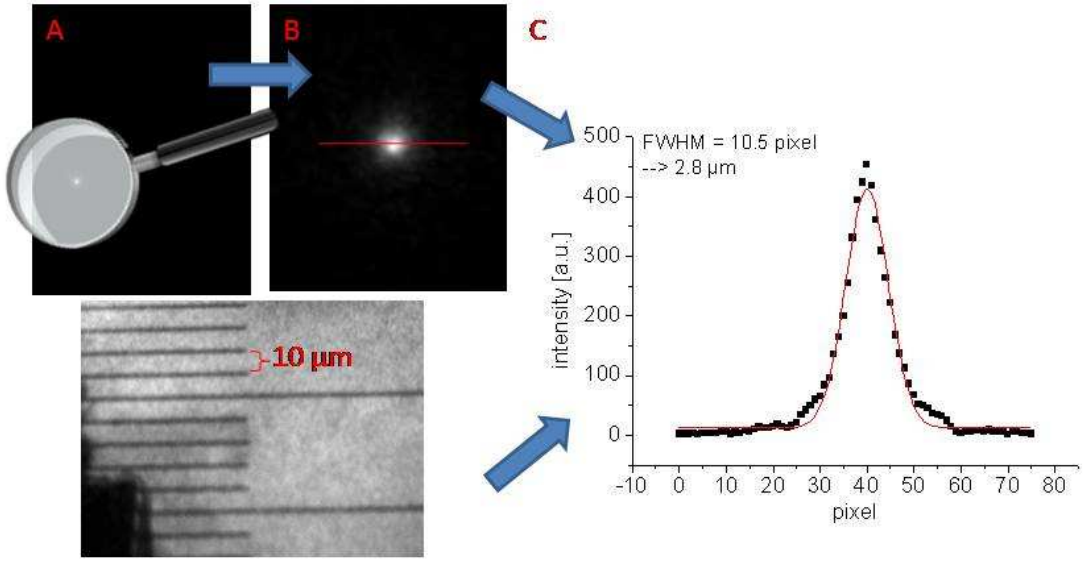

Figure 4.8: Determination of spatial resolution of the 2c2p microscope. A shows the fluorescence image of the focus. In B a line is laid through this focus. Along this line the intensity profile shown in C is measured. A transmitive image of an object micrometer gives the scale. Here one camera pixel corresponds to 266 nm object size. This leads to a spatial resolution of only 2,8 µm.

Figure 4.8 A shows the image of a 2c2p focus of the 100x objective. Plotting the intensity profile along the shown line and plotting it with a Gaussian function renders a FWHM value of the focus of 10.5 pixels. With respect to the image of the object micrometer at the same magnification this corresponds to a resolution of only 2.8 µm.

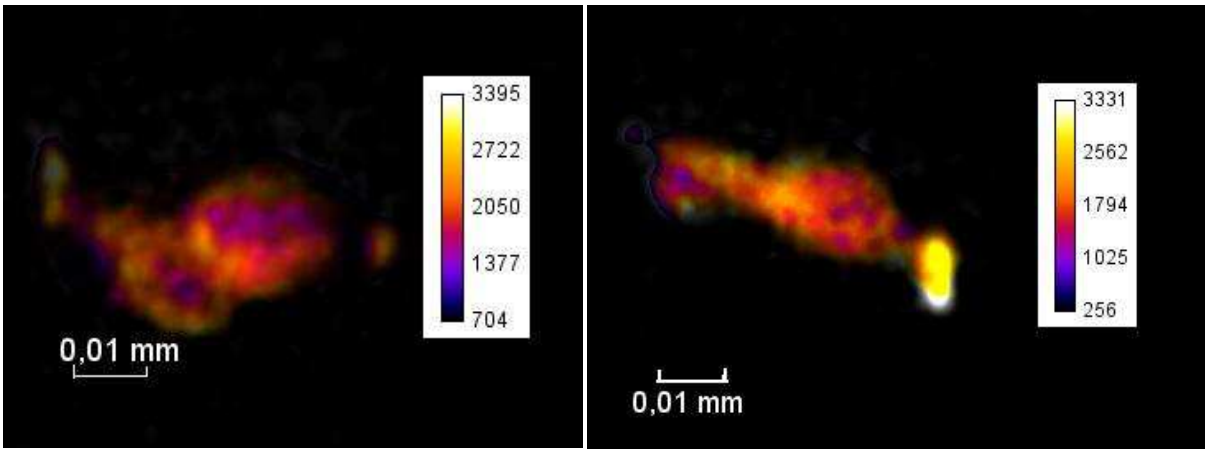

Figure 4.9: 2c2p FLIM pictures of MIN6 cell cultures acquired with the beam-scanning microscope setup combined with time gated camera detection. The picture's brightness corresponds to fluorescence intensity while the color encodes the fluorescence lifetime of a best fit of a mono exponential decay. The raw images are deconvoluted using the image of the focus as 2D point spread function acquired with the camera. Software used is imageJ 1.41e, National Institute of Health, USA, public domain.

Figure 4.9 shows fluorescence lifetime images of the 2c2p auto fluorescence of MIN 6 cells taken with this setup. The images illustrate the poor resolution of only 2.8 µm. Details of the cells can hardly be seen. Only the nuclei of the cells are slightly pronounced. The color code of the image corresponds to a mono exponential decay. It has to be noted that due to the quality of the low signal it was not reasonable to perform a multi exponential fit to the data.

Implementing a magnification lens system leads to less blurred images but for the cost of signal intensity per pixel because the same number of photons is spread over a wider area of the MCP. Longer acquisition times are the consequence. Figure 4.10 shows corresponding measurement that of figure 4.8 but this time a fourfold magnification in front of the intensifier is used.

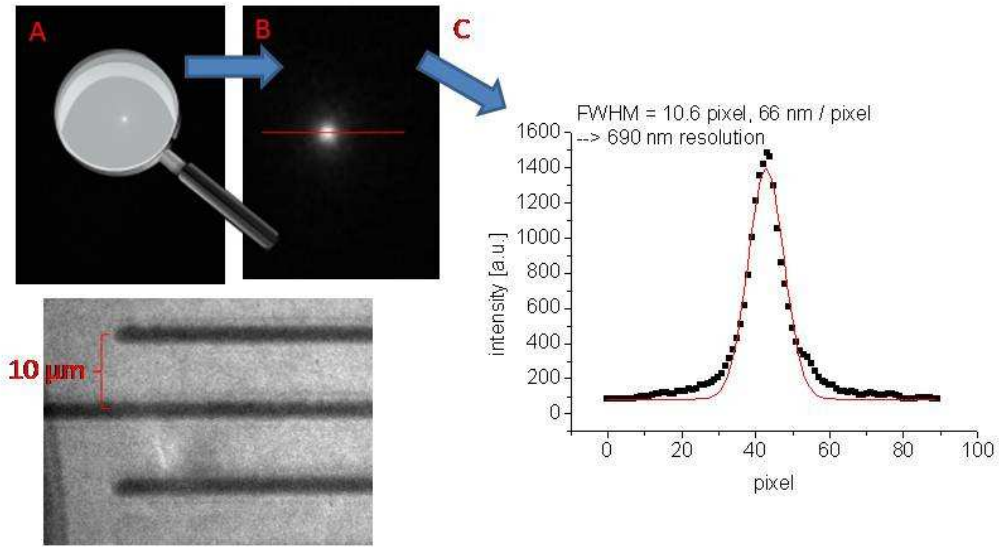

Figure 4.10: After introduction of a 3 cm quartz lens a fourfold magnification is achieved. Now one pixel corresponds with 66 nm. By projecting the fluorescence of the focus on a larger area of the MCP the blur effect is reduced. Now a spatial resolution of 690 nm is achieved.

Again the image of the focus has a FWHM value of about 10 pixels. But at this magnification one pixel correlates with only 66 nm, according to the image of the object micrometer. indicates a spatial resolution of now 690 nm. Still, this value is too high for a multi photon excitation using 800 nm and 400 nm light. The theoretical value according to Abbe`s law should lie well below 200 nm.

Chromatic aberrations are problematic in VIS microscopy. Arising from different diffraction indices at different wavelengths, they increase dramatically when spectrally moving to the UV because there the diffraction index increases disproportionally high with shorter wavelengths. Additionally, achromatic optics for these wavelengths are not available at affordable cost.

In conclusion, the camera system is suitable for 2c2p applications where very high spatial resolution is not necessary and, consequently, low magnifications can be used. The relatively low quantum yield of the camera system is compensated by the fact that fluorescence photons from relative large scanning areas of the sample are projected on each pixel. Hence, acquisition times of 20 to 30 seconds can be realized for image acquisition of low resolution 2c2p auto fluorescence images of MIN6 cells. A FLIM series of 20 images then takes approximately 6 to 10 minutes. With the magnification in place this time has to be multiplied by the square of magnification factor. Such a 16 fold prolonged acquisition time is not suitable for cell imaging anymore. Additionally, the background noise of the camera system at

this acquisition time is so high that the signal to noise ratio is near one. For this reason the experimental setup of the microscope was changed to a different detection and scanning mode.

An established method for accelerating camera based multi photon fluorescence microscopy is the use of parallel scanning with multiple beams which will be an option for 2c2pLSM at a later stage of development.[30] This method can provide more fluorescence intensity which allows reducing the acquisition times. Then the implementation of a sufficient magnification becomes possible.

4.3.2 Sample scanning setup with APD

To enhance the sensitivity and spatial resolution of the microscope the scanning mode and the detection system was changed. Instead of scanning the laser beams and, thus, the foci across the sample, the sample is scanned via a piezo driven table (Physik Instrumente GmbH, Karlsruhe) while the two overlapping foci stay at a fixed position under the objective. Additionally to the complementary scanning modes the two setups follow different fluorescence detection techniques. Fluorescence is now detected using an avalanche photo diode (APD) (MPD Micro Photon Devices, Bolzano, Italy) in a non-descanned position. The signal from the APD is processed by time correlated single photon counting (TCSPC) device (Picoharp 300, PicoQuant GmbH, Berlin) which also controls the piezo table. Data acquisition is achieved using the corresponding PicoQuant software SymPhoTime.

While the PicoStar camera system using the time gated method detects only photons arriving in the preset detection time window (gate) the TCSPC APD combination detects every incoming photon registered by the APD at any time. When a photon is detected its time of arrival is stored. After a measurement the histogram of arrival times can be plotted to give the fluorescence decay curve. Integration over the whole detection time allows displaying intensity only pictures.

Modern TCSPC systems like the one used in these experiments are able to count photons with average rates of 5 mega counts per second (MCPS). This corresponds to a dead time of only 200 ns. This enables the system to register a photon after every 16^{th} laser pulse making TCSPC suitable even for strong fluorescence applications.

In addition to the enhanced photon efficiency, the spatial resolution is far less decreased by scattering in turbid media compared to detection with a camera. In a non-descanned detection mode the whole fluorescence collected by the objective is focused onto a single spot detector, here the APD. Scanning the sample pixel by pixel and storing the measured intensity, the spatial resolution is only limited by the resolution of the exciting laser beam and not by the imaging quality of the fluorescence light. This is especially advantageous in scattering media. In a non-descanned setup most of the scattered fluorescence photons are also projected onto the detector.[30]

Acquisition times for cell images using 2c2p excitation of intrinsic protein fluorescence are dependent on the image size. Typical times are in the range of 10 to 30 minutes. Hence, increasing the photon efficiency will be one of the major challenges for further development of the 2c2pLSM.

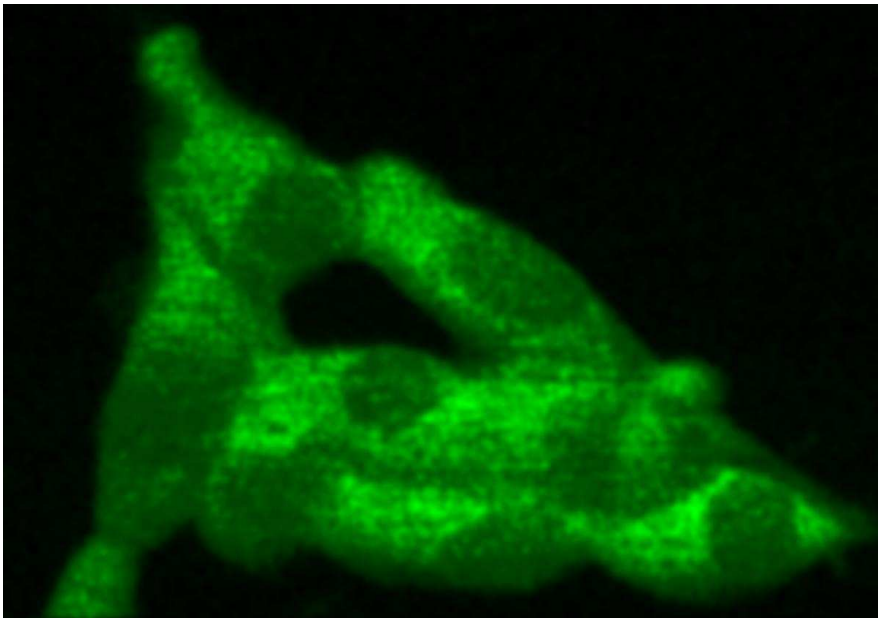

Figure 4.11: 2c2pLSM image of MIN 6 cells using the TCSPC sample scanning setup. Compared with the image from the camera the increased resolution is apparent.

4.4 References for chapter 1 - 4

[1] H. Shuman, J. M. Murray, C. DiLullo *Biotechniques*. **1989**, 7, 154-163.

[2] W. Denk, J. H. Strickler, W. W. Webb *Science, New Series*. **1990**, 248, 73-76.

[3] F. Helmchen, W. Denk *Nautre Methods*. **2005**, 2, 933-940.

[4] R. Heintzmann, P. A. Benedetti *Appl. Opt.* **2006**, 45, 5037-5045.

[5] D. Karadaglić, T. Wilson *Micron*. **2008**, 39, 808-818.

[6] K. I. Willig, R. R. Kellner, R. Medda, B. Hein, S. Jakobs, H. S. W. *Nature Methods*. **2006**, 3, 721-723.

[7] B. R. Rankin, R. R. Kellner, S. W. Hell *Opt. Lett.* **2008**, 33, 2491-2493.

[8] A. Egner, C. Geisler, C. v. Middendorff, H. Bock, D. Wenzel, R. Medda, M. Andresen, A. C. Stiel, S. Jakobs, C. Eggeling, A. Schönle, S. W. Hell *Biophys. J.* **2007**, 93, 3285-3290.

[9] R. Heintzmann, G. Ficz *Brief Funct Genomic Proteomic*. **2006**, 5, 289-301.

[10] P. R. Monson, W. M. McClain *J. Chem. Phys.* **1971**, 56, 4817-4825.

[11] J. R. Lakowicz, I. Gryczynsiki, H. Malak, Z. Gryczynski *Photochem. Photobiol.* **1996**, 64, 632-635.

[12] K. M. Marks, G. P. Nolan *Nature Methods*. **2006**, 3.

[13] R. Y. Tsien *Biochemistry*. **1980**, 19, 2396-2404.

[14] P. H. Hai-Jui Lin, Jung Sook Kang, Joseph R. Lakowicz. **2001**.

[15] H. S. Hai-Jui Lin, Joseph R. Lakowicz *Analytical Biochemistry*. **1999**, 269, 162-167.

[16] R. Y. Tsien *Annu Rev Biochem*. **1998**, 67, 509-544.

[17] J. M. Tavare, L. M. Fletcher, P. B. Oatey, L. Tyas, J. G. Wakefield, G. I. Welsh *Diabetic Medicine*. **2001**, 18, 253-260.

[18] A. A. H. Shaohui Huang, Watt W. Webb *Biophysical Journal*. **2002**, 82, 2811–2825.

[19] J. R. Lakowicz, Principles of fluorescence spectroscopy Kluwer Academic/Plenum Publishers, New York, **2006**.

[20] J. R. Lakowicz, I. Gryczynski *Biophys. Chem.* **1992**, 45, 1-6.

[21] M. Hellings, M. De Maeyer, S. Verheyden, Q. H. Els, J. M. Van Damme, W. J. Peumans, Y. Engelborghs *Biophys. J.* **2003**, 85, 1894-1902.

[22] A. V. Ostrovsky, L. P. Kalinichenko, V. I. Emelyanenko, A. V. Klimanov, E. A. Permyakov *Biophys. Chem.* **1987**, 30, 105-112.

[23] Y. Engelborghs *Journal of Fluorescence*. **2003**, 13, 9-16.

[24] M. K. Kuimova, G. Yahioglu, J. A. Levitt, K. Suhling *J Am Chem Soc*. **2008**, 130, 6672-6673.

[25] R. Niesner, B. Peker, P. Schlüsche, K. H. Gericke, C. Hoffmann, D. Hahne, C. Müller-Goymann *Pham Res*. **2005**, 22, 1079-1087.

[26] R. K. Benninger, Y. Koç, O. Hofmann, J. Requejo-Isidro, M. A. Neil, P. M. French, A. J. DeMello *Anal. Chem.* **2006**, 78, 2272-2278.

[27] G. R. Fleming, J. M. Morris, R. J. Robbins, G. J. Woolfe, P. J. Thistlethwaite, G. W. Robinson *Proc. Natl. Acad. Sci. USA*. **1978**, 75, 4652-4656.

[28] N. Vekshin, M. Vincent, J. Gallay *Chem. Phys. Let.* **1992**, 199, 459-464.

[29] Y. Engelborghs *Spectrochimica Acta*. **2001**, 57, 2255-2270.

[30] R. Niesner, V. Andresen, J. Neuman, H. Spieker, M. Gunzer *Biophys. J.* **2007**, 93, 2519-2529.

5 Two-Color Two-Photon Excitation using femtosecond Laser Pulses

5.1 ABSTRACT

The use of two-color-two-photon (2c2p) excitation easily extends the wavelength range of Ti:Sa lasers to the UV widening the scope of its applications especially in biological sciences. We report observation of 2c2p excitation fluorescence of p-terphenyl (PTP), 2-methyl-5-t-butyl-p-quaterphenyl (DMQ) and tryptophan upon excitation with 400 and 800 nm using the second harmonic and fundamental wavelength of a mode locked Ti:Sa femtosecond laser. This excitation is energetically equivalent to a one photon excitation wavelength at 266 nm. The fluorescence signal is only observed when both wavelengths are spatially and temporally overlapping. Adjustment of the relative delay of the two laser pulses renders a cross correlation curve which is in good agreement with the pulse width of our laser. The fluorescence signal is linearly dependent on the intensity of each of the two colors but quadratically on the total incident illumination power of both colors. In fluorescence microscopy the use of a combination of intense IR and low intensity blue light as a substitute for UV light for excitation can have numerous advantages. Additionally, the effect of differently polarized excitation photons relative to each other is demonstrated. This offers information about different transition symmetries and yields deeper insight into the two-photon excitation process.

5.2 Introduction

In recent years two-photon laser scanning microscopy (2pm) [2] has become an indispensable tool especially for biological science as the use of more than one photon provides numerous advantages. First of all separation of excitation and fluorescence light is much easier because of the larger difference in wavelength compared to conventional confocal microscopy. Therefore better signal to noise ratios and high contrast pictures can be obtained. Secondly the usage of IR excitation light instead of UV/Vis light leads to reduced photo damage and higher penetration depth[30] in biological tissue due to lower absorption coefficients in the IR region[31] than in the visible which is usually used for confocal microscopy. Additionally, due to the quadratic dependence on the intensity, excitation in 2pm is limited to the focal area only. Thus, out of focus excitation is avoided leading to limited photo damage and an intrinsic

3D resolution. Most common excitation sources for 2pm are Ti:Sa lasers. The femtosecond (fs) pulses from these lasers are almost ideal for this purpose as they combine high excitation power during the pulse, which is essential for a good excitation yield[32], with low energy deposition to the sample preventing it to be photo damaged. Furthermore, pulsed excitation furnishes the basis for excellent time resolution using time gated[33] or time correlated single photon counting (TCSPC)[34] detection systems. Hence, a variety of time resolved fluorescence techniques as Fluorescence Lifetime Imaging (FLIM)[33, 35-37] or Fluorescence Anisotropy Imaging (Tr-FAIM)[36] have been established.

Typically 2pm and other spectroscopic two photon methods are performed almost exclusively using two excitation photons of the same wavelength. Only very few attempts have been made so far to extend these methods to two-color two-photon excitation.[11, 38, 39] This is asurprising as the use of two photons at different wavelength for excitation offers the opportunity to extend the wavelength range where the Ti:Sa laser can be used under retention of all advantages of two-photon excitation. According to theoretical considerations, spatial resolution[40] and penetration ability[41], depending on the microscopical setup, are expected to improve for 2c2p excitation compared to confocal or conventional 2pm microscopy, respectively.

Using the fundamental and second harmonic of a Ti:Sa 2c2p excitation in the UV can be achieved. As modern mode locked fs-lasers offer a tunable range from about 700 nm to 1000 nm the conventional 1c2p technique excites fluorophores in a spectral range of about 350 nm to 500 nm. With 2c2p an additional spectral window from about 230 nm to 330 nm is at hand extending the wavelength range of the Ti:Sa laser to the UV where e.g. tryptophan, a fluorescent amino acid responsible for protein fluorescence[20, 27], can easily be excited. Furthermore, this spectral window corresponds to the excitation wavelength of DNA[42].

In addition, 2c2p excitation offers a unique opportunity of getting a deeper understanding of two photon absorption processes. Here, in contrast to 1c2p experiments, it is possible to manipulate the polarization of each of the absorbed photons independently. Theoretical considerations[37, 43] as well as 2c2p experiments conducted as absorption measurements[10] imply that there is a close relationship between the relative polarizations of the two photons and the symmetry of the involved electronic states. The absorption data published by McClain[10, 43] lead to the assumption that it should be possible to discriminate chromophores possessing different symmetries by their different behavior towards different excitation polarizations. Additional indication for this assumption is given by the work of Lakowicz[38]

et. al. where a different behavior of PTP and indole towards the excitation with perpendicularly polarized photons was found. The effect of circularly polarized photons is still unclear.

To the best of our knowledge, we present the first observation of 2c2p excitation fluorescence using a modern passive mode locking Ti:Sa laser source emitting fs pulses. The fundamental and second harmonic of a Ti:Sa laser are focused confocally through a lens into a cuvette where fluorescence is observed as a result of 2c2p excitation. The phenomenon is observed for PTP, DMQ and tryptophan.

Furthermore we present the first fluorescence lifetime measurements performed in the time domain studying 2c2p excitation fluorescence and, in addition, the behavior for different linearly and circularly polarized photons.

5.3 Material and Methods

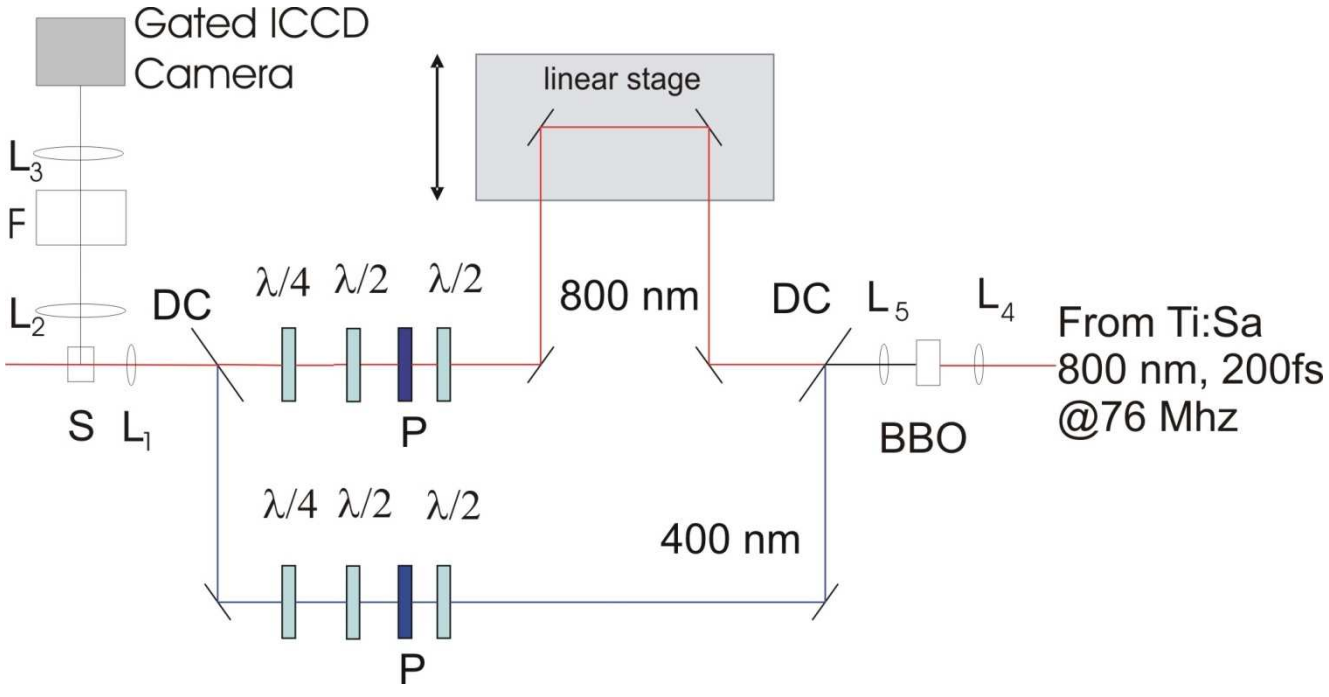

Figure 5.2. Experimental setup. BBO = bariumborate crystal for frequency doubling, L = lens, DC = dicroic mirror, □/2 = half wave plate, □/4 = quarter wave plate, F = set of filters (Semrock NF01-405U, Semrock NF01-808U both at 10° angle, Schott UG 11 and a interference filter 340/80 nm).

The fs laser pulses are provided by a Ti:Sa laser (Mira 900B, Coherent) which is pumped by a Nd:YVO4 solid state laser (Verdi V10, coherent). The Ti:Sa is operated at 800 nm with a pulse width of 200 fs. The initial 800 nm beam is frequency doubled using a beta-bariumborate (BBO) crystal (figure 5.1). The two colors, i.e. the frequency doubled and the remaining fundamental light, are then separated by a dichroic mirror so that blue and red light can be manipulated independently in terms of power, polarization and optical path length. Power adjustment is realized using a set of a λ/2 plate (all wave plates: quartz, low order, coated) and a thin layer polarizer (P) for each beam. All states of linear and circular polarization can be prepared for each color separately using a set of λ/2 and λ/4 plates. The degree of polarization for linear and circular case are measured using an analyzer and a power meter for the linear case and a set of Fresnel Rhomb, polarizer and power meter for the circular case, respectively. All degrees of polarization used for the measurements are in the range of 95-99%. The optical path length of the 800 nm light can be adjusted using a delay line in the red path consisting of two mirrors mounted to a precise linear stage to provide temporal overlap (figure 5.2).

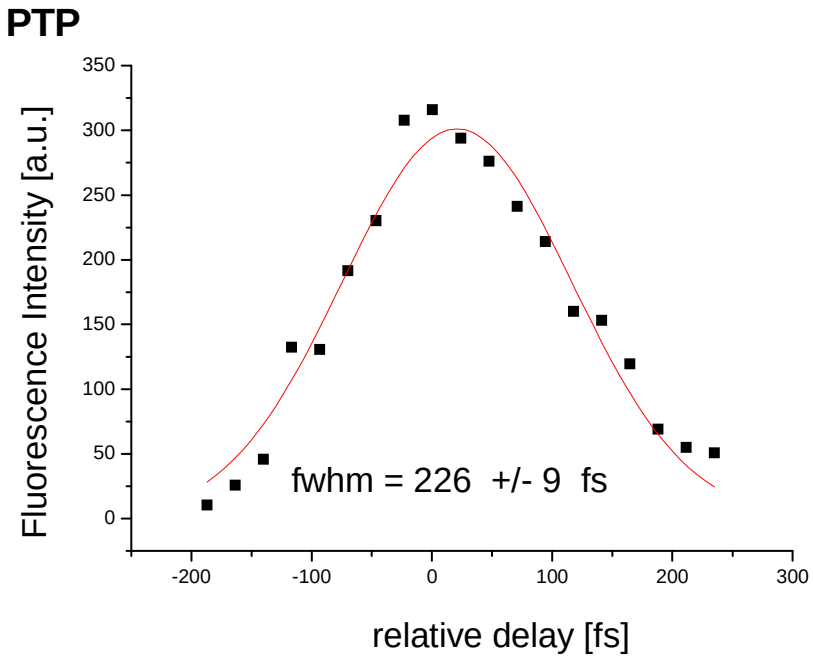

Figure 5.2. Cross correlation curve showing the dependence of the fluorescence intensity on the temporal overlap. The resulting fwhm value is in good agreement with the pulse width of the laser.

After reunion of the two colors by a second dichroic mirror both beams are focused in a confocal setup through an achromatic lens with 5 cm focal length into the sample located in a 5x5 mm cuvette. For adjustment this cuvette can be replaced by a pinhole or a second BBO crystal for accomplishing spatial and temporal overlap, respectively. Temporal overlap is indicated by wave mixing of the 800nm and 400 nm beams resulting in 266 nm emission from the crystal.

Fluorescence is monitored in a perpendicular setup through a set of filters consisting of UG 11 (Schott), 340/80 nm interference filter, and two 400 and 800 nm notch filters (Semrock) and detected by a time gated ICCD camera system (picostar, LaVision GmbH, Göttingen). The gate width of the camera system can be adjusted from 200 ps to 1 ns and, in combination with a delay generator (Kentech Instruments Ltd.), a time resolution as good as 10 ps can be achieved[44].

PTP and DMQ were purchased from Lamda Physik AG, Germany, and used without further purification. PTP and DMQ were dissolved in cyclohexane to give 1 mM solutions. Tryptophan was purchased from Sigma-Aldrich to prepare a 1 mM solution in PBS buffer.

5.4 Results

Two-color two-photon fluorescence was studied for different dyes. First observations were made for PTP in order to have comparable results with respect to previous publications[11] using picosecond dye lasers. After this comparison we studied other dyes where 2c2p fluorescence is unknown. We found clear evidence for 2c2p excitation to be the origin of the detected fluorescence of PTP, DMQ and tryptophan. The most straight forward observation is that the full fluorescence signal is only present when the sample is illuminated by both laser beams and only when they temporarily overlap.

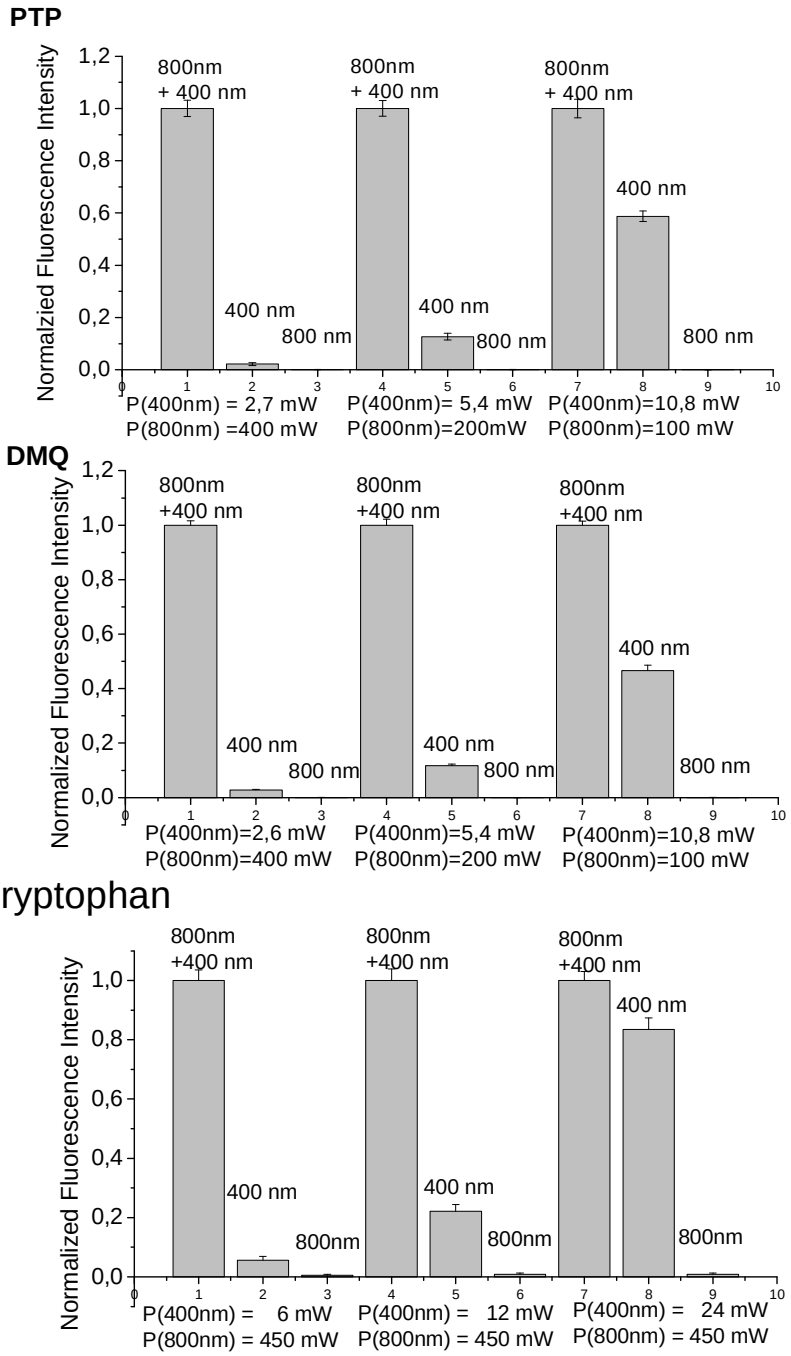

Figure 3. Fluorescence intensity for irradiation by one or two laser beams at different power ratios of the 400 nm and 800 nm light. Highest fluorescence intensities are observed for irradiation with both colors. 400 nm alone produces a fluorescence signal from 1c2p excitation. This can be suppressed by using few 400 nm light and much 800 nm light as 800 nm light alone produces no signal even at high intensities. Each data point represents the mean value of 20- 30 measurements and the error bars show the standard deviation.

As shown in figure 3 strong fluorescence is only observed when both beams are irradiated into the sample. The columns labeled 800 nm + 400 nm represent the 2c2p fluorescence signal which is obtained by subtracting the signals for each color alone from the signal which is present when both beams are irradiated. For better comparison the data were normalized to the 2c2p signal. Using 400 nm exclusively, we observe a weak fluorescence signal. Further investigations of the fluorescence from the blue excitation light alone showed a quadratic dependence of the fluorescence intensity on the excitation power (figure 5.4).

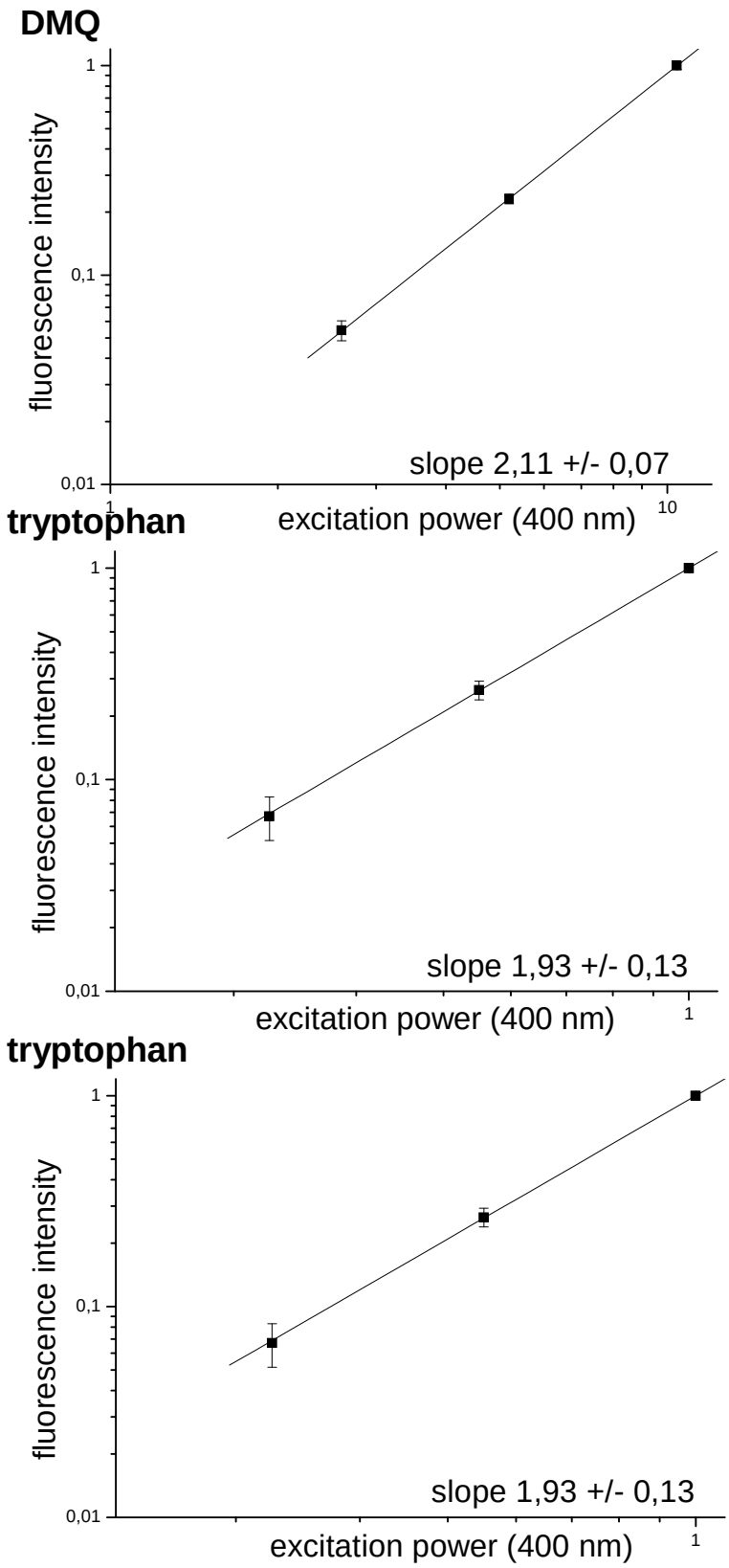

Figure 4. Dependence of the fluorescence intensity on the excitation power when only 400 nm light is irradiated. The quadratic dependence indicates a one-color two-photon excitation (1c2p).

This indicates a one-color two-photon (1c2p) absorption being the origin of that fluorescence. This assumption is in good agreement with the one photon absorption spectra[19, 45] which all show a strong second absorption band around 200 nm. However, in all cases almost no signal is detected for irradiation of 800 nm only. As can be seen from figure 5.3 attenuation of the blue beam with simultaneous increase of the power of the red beam easily allows suppressing the undesired 1c2p signal with retention of the 2c2p fluorescence intensity. This is possible because in case of a two-photon absorption the absorption rate is linearly dependent on the product of the intensities of each color.

$$\frac{dN}{dt} = -\delta \cdot I_{800\,nm} \cdot I_{400\,nm} \cdot N \qquad (1)$$

With N = Nummber of Molecules in ground state, δ = two photon absorption cross section, I = photon flux.

Therefore the fluorescence intensity is expected to be linearly dependent on each of the excitation intensities providing the other is held constant. If the power of the 400 nm beam is attenuated, the 2c2p signal will decrease proportional while the 1c2p signal will decrease more rapidly because of its quadratic dependence. If the power of both colors is adjusted one expects a quadratic dependence on the total power of both colors. The data shown in (figure 5.5) indicate that our experimental results are in very good agreement with these considerations.

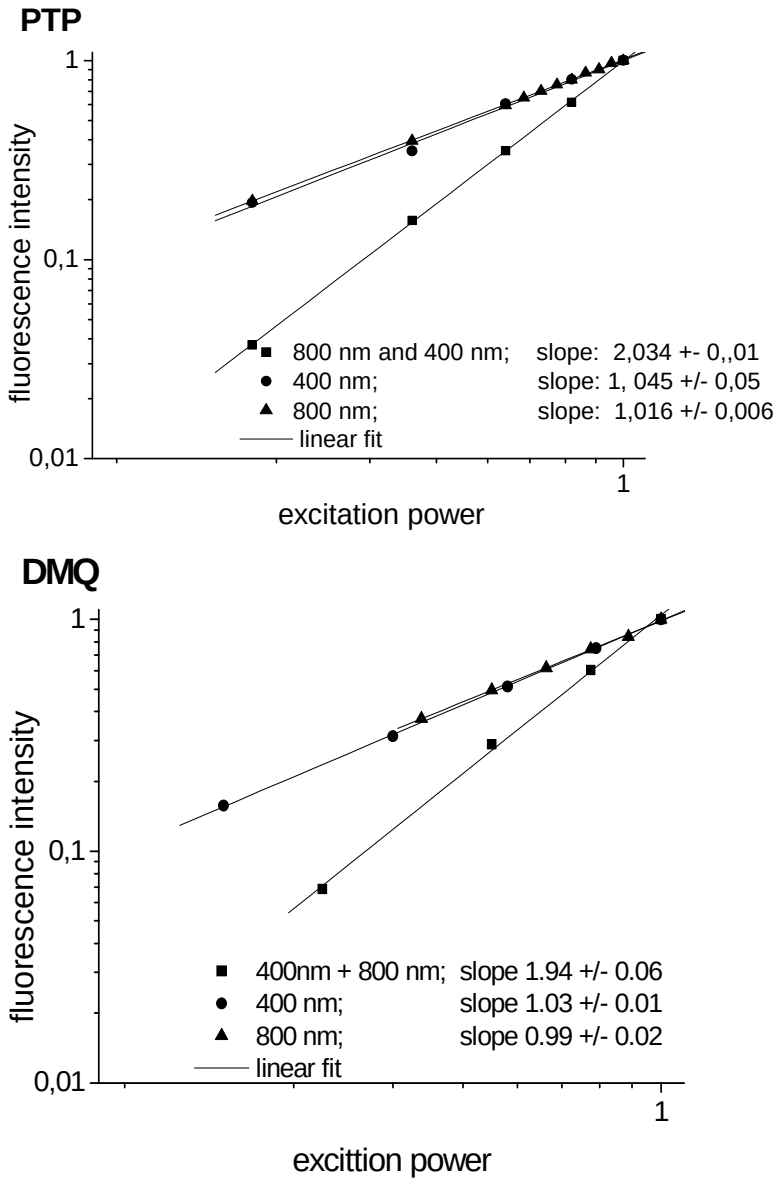

Figure 5.5. Dependence of 2c2p fluorescence intensity on variation of the power level of one or both colors. If the power of only one color is changed, a linear dependence is found. For simultaneous variation of the power of both colors a quadratic dependence on the total excitation intensity is found.

For all dyes and different power levels a three photon excitation is not observed although for 800 nm irradiation this would be energetically equivalent to a 2c2p excitation with 800nm and

400 nm. It seems that much higher intensities would be necessary because of the extremely small three photon absorption cross sections.

Another confirmation for the presence of 2c2p excitation is a cross correlation experiment where the time delay between both laser pulses is varied. As both photons are required for the 2c2p excitation the maximal fluorescence intensity is expected only when both laser pulses are exactly temporally overlapping. As expected, this experiment renders a cross correlation curve (figure 5.2) whose FWHM value of 226 +/- 9 fs is in good agreement with the pulse width of the Ti:Sa laser in this experiment.

The pulse width of the 800 nm light was measured after the second dicroic morror rendering an autocorrelation curve with an fwhm value of 260 fs. Assuming gaussian pulse shape this corresponds to a pulse width of $(260\,fs)/\sqrt{2} = 184\,fs$. Hence the pulse width of the blue light can be expected to have a pulse width of $(184\,fs)/\sqrt{2} = 130\,fs$ for a quadratic dependence of the SHG on the 800 nm power. Therefore, the expected value for a cross correlation of these two pulses is $\sqrt{((130fs)^2 + (184fs)^2)} = 225\,fs$ endorsing the measured value of 226 +/- 9 fs.

To confirm that the 2c2p excitation leads to fluorescence emission from the S1 state fluorescence lifetimes were measured (figure 5.6) using a time gated intensified camera system.

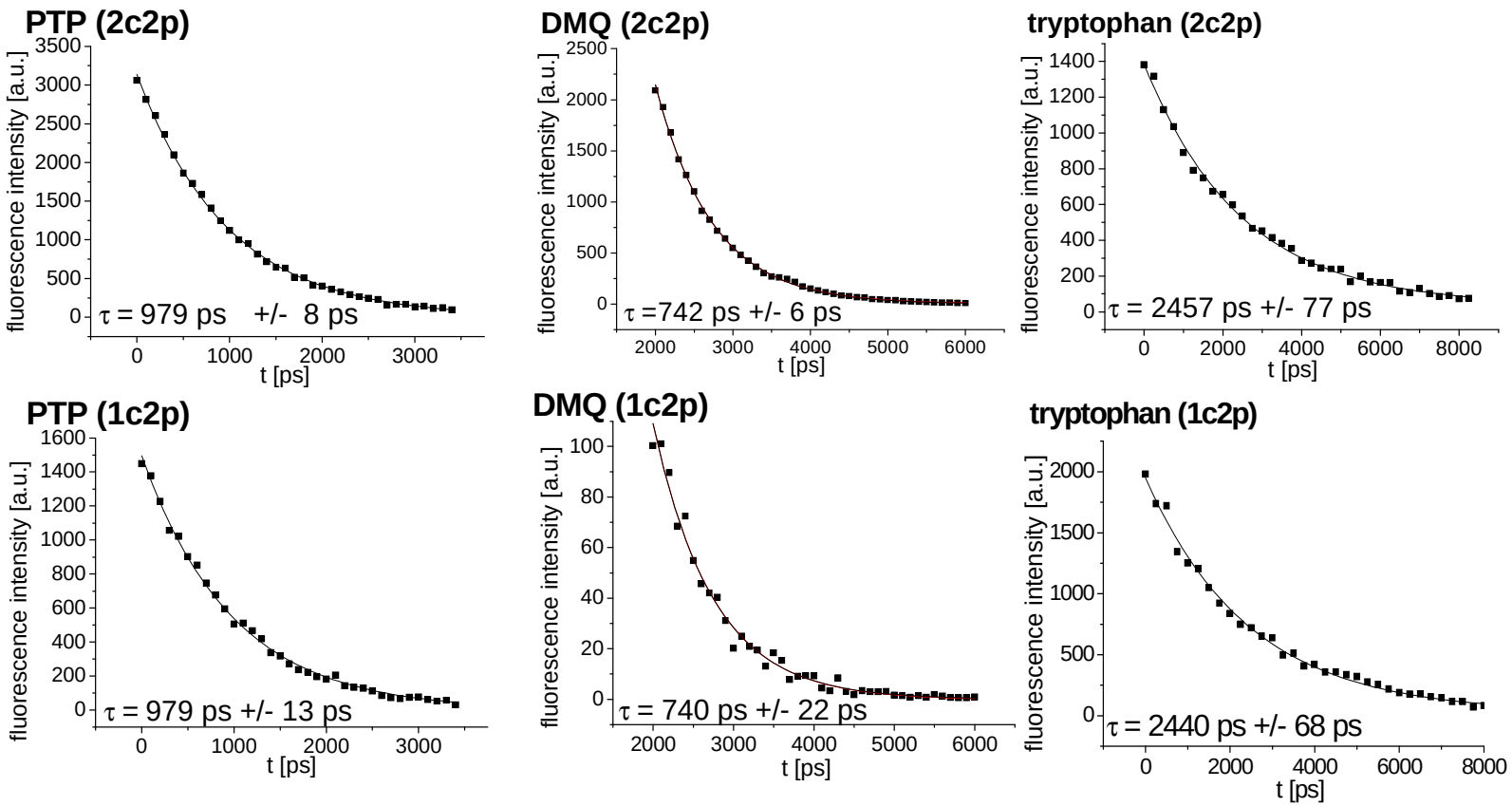

Figure 5.6. Fluorescence lifetimes of PTP, DMQ and tryptophan for 2c2p and 1c2p excitation. For both modes of excitation similar lifetimes are found indicating that fluorescence emission occurs from the same excited state for both types of excitation. A mono exponential decay is used for fitting the data.

All observed lifetimes are in good agreement with those known from literature[46, 47] [48]for an one photon excitation. Additionally, we found no difference in fluorescence lifetime for 1c2p or 2c2p excitation. Thus, it can be concluded that the origin of the fluorescence is the same electronic state, i.e. the S1 state.

The effect of differently polarized excitation photons on the fluorescence intensity is also investigated. As shown in figure 5.7 a change from two parallel polarized photons (r ls b ls) to two perpendicular photons (r ls b lp) results in a reduction of fluorescence intensity to approximately 40% of the parallel case. For excitation with two circular polarized photons (r cr b cl and r cr b cr) we also find reduced fluorescence intensities. As can be seen from figure 7 the intensities resulting from circular polarization are higher than those from linear polarized photons being oriented perpendicular to each other but still smaller than from the parallel case. We could not find a significant difference for circular polarized photons with same (r cr b cr) or opposite (r cr b cl) sense of rotation. The differences in fluorescence intensities are influenced by the symmetry of all involved electronic states. In case of a two-photon absorption this means, that the virtual states have a contribution to this effect, too. A detailed theory allowing conclusions from the measured polarization dependency on the symmetry of the molecule requires advanced theoretical analysis which needs to be done.

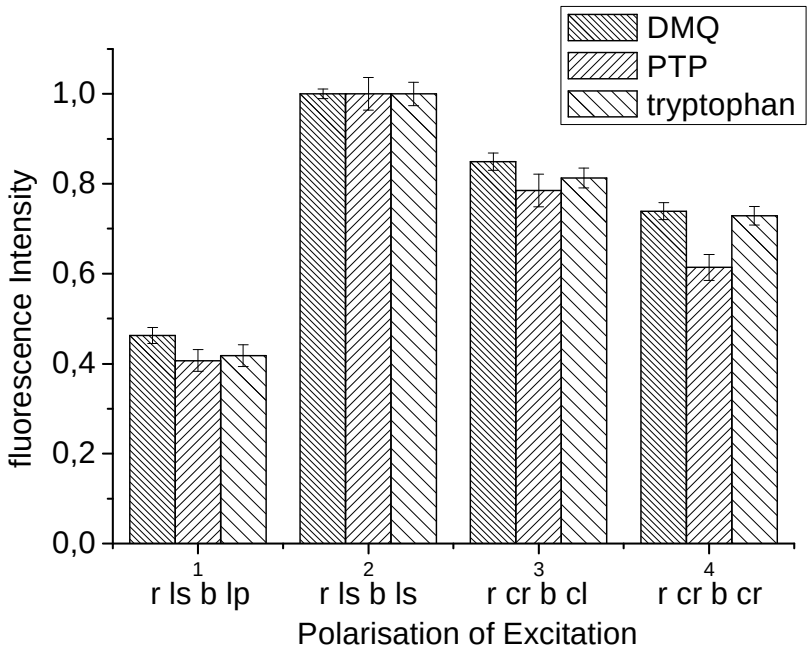

Figure 5.7. Influence of the relative polarization of the exciting photons on the fluorescence intensity. Two linearly polarized photons which are parallel lead to maximum fluorescence where as two linearly polarized photons with an angle of 90° between the polarizations lead to the weakest fluorescence signal. Circularly polarized photons lead also to reduced fluorescence signal compared to two parallel photons. r = red light, b = blue light, ls = linear perpendicular polarized, lp = linear parallel polarized, cr = circular polarized with right sens of rotation, cl = circular polarized with left sense of polarization.

5.5 Discussion

Two color two-photon excitation is a powerful tool for enlarging the spectral range of nowadays fs-Ti:Sa laser systems being used for spectroscopy and two-photon microscopy. We demonstrate measurements of 2c2p excitation fluorescence using fs-pulses from a Ti:Sa laser. Since these experiments were carried out using a time gated camera system as a detector which is normally used for fluorescence lifetime imaging, we believe that applications of 2c2p excitation to microscopy is now within reach. The use of fs-pulses instead of ps-pulses has several advantages, although the securing of temporal overlap is definitely more challenging the shorter the pulses become. For multi photon processes high excitation powers are desired as the rate of absorption is dependent on the square of the total photon flux used for excitation in combination with very small multi-photon absorption cross sections. On the other hand the amount of energy introduced into the sample should be as low as possible to

avoid damage. The solution for this dilemma is the use of pulses as short as possible. [32] The ideal light source for ultra short pulses today is the Ti:Sa laser emitting fs-pulses in high repetition and high power output. Our experiments show that even with fs-pulses it is possible to have stable spatial and temporal overlap in an experimental setup. Furthermore, it is worth mentioning that the implementation of 2C2P excitation into a microscope will lead to a much higher photon efficiency. First of all the higher focusing of a high numeric aperture objective will result in increased photon fluxes in the focal region. As the excitation rate is quadratically dependent on the photon flux this will lead to a much more efficient excitation. Secondly a higher fraction of the occurring fluorescence photons is collected again, due to the high numeric aperture. Considering both effects, one can conclude that observation of 2C2P excitation fluorescence in a microscope will be about two orders of magnitude more efficient than in the present experimental setup. In other words for achieving the the same signal intensity only about one percent of the excitation power is required.

The results of 2c2p excitation of PTP were in good agreement with those from previous publications where measurements have been performed using cavity dumped ps dye lasers.[11] In addition, with DMQ and tryptophan we found two other dyes suitable for 2c2p excitation using 800 nm and 400 nm for excitation which have not been studied with 2c2p excitation yet. All fluorophores show good 2c2p excitation fluorescence. They also show some 1c2p excitation fluorescence, however, only when strong blue light is applied. Therefore it seems crucial to use an excess of red light with only few of the blue component. What on first sight looks like a disadvantage turns out to be concurrent with one of the big advantages of 2c2p excitation. In fact for most applications it will be highly desired to use only low level 400 nm light to keep photo damage low. The fact that the fluorescence intensity is linearly dependent on the product of the intensities of both colors offers the possibility of maintaining a high penetration depth in combination with low photo damage compared to one-photon UV excitation. The low power of the blue light can easily be compensated by increasing the power of the IR light which is much less harmful to biological samples. The IR can easily penetrate through biological tissue without being absorbed and therefore it will not inflict much damage, as experiences with common 2pm show.

To study the proposed influence of different relative polarizations on the excitation of molecules with different symmetries it is crucial to have a good variety of different dyes.

So far we found no evidence for such an influence for the studied molecules. The reason might be the similar symmetry of the involved transitions. Future time and polarization

resolved measurements will render more detailed information on the anisotropic character of the fluorescence decay. So one can expect that two photons being not parallel polarized, as it is the case for 1c2p excitation, to give a significantly different photo selection. This will influence the observed initial anisotropy after excitation.

Besides, these theoretical considerations the demonstration of tryptophan as a suitable fluorophore for 2c2p excitation will offer a good variety of possible applications. Tryptophan can be found in lots of different proteins and 2c2p excitation will allow to use it as a natural fluorescent tag as well as a fluorescent probe inside the protein without applying UV to proteins. Hence, the advantages of label free measurements and advantages of high time resolution resulting from pulsed excitation with the Ti:Sa will be combined and additionally enriched by the fact that direct UV irradiation is avoided and therefore photo damage can be reduced. Although 2c2p fluorescence from tryptophan is roughly 20 times weaker than from the other dyes, it is still sufficient for fluorescence analysis. Experiments concerning protein bioassays are in progress.

5.6 Conclusion

We demonstrated that 2c2p excitation with fs lasers is an option for extending their spectral range in combination with advantages arising from the use of multi photon excitation. The ultra short fs-pulses are an ideal basis for later application in microscopy. Within the newly gained spectral range tryptophan can be 2c2p excited and used as fluorophore.

5.6.1 Acknowledgement

This work was supported by the Bundesministerium für Bildung und Forschung (BMBF) under grant 0313412C.

5.7 References

[1] W. Denk, J. H. Strickler, W. W. Webb *Science, New Series*. **1990**, 248, 73-76.

[2] R. Niesner, V. Andresen, J. Neuman, H. Spieker, M. Gunzer *Biophys. J.* **2007**, 93, 2519-2529.

[3] R. Weissleder, V. Ntziachristos *Nature Medicine*. **2003**, 9, 123-128.

[4] R. Niesner, W. Roth, K.-H. Gericke *Chem. Phys. Chem.* **2004**, 5, 678-687.

[5] D. Elson, J. Requejo-Isidro, I. Munro, F. Reavell, J. Siegel, K. Suhling, P. Tadrous, R. Benninger, P. Lanigan, J. McGinty, C. Talbot, B. Treanor, S. Webb, A. Sandison, A. Wallace, D. Davis, J. Lever, M. Neil, D. Phillips, G. Stamp, P. French *Photochem. Photobiol. Sci.* **2004**, 3, 795-801.

[6] W. Becker, A. Bergmann, G. Biscotti, A. Rück *Proc. Spie.* **2004**, 5340, 1-9.

[7] E. Gratton, S. Breusegem, J. Sutin, Q. Ruan, N. Barry *Biomed. Opt.* **2003**, 8, 381-390.

[8] K. Suhling, P. M. W. French, D. Phillips *Photochem. Photobiol. Sci.* **2005**, 4, 13-22.

[9] W. M. McClain *J. Chem. Phys.* **1972**, 58, 324-326.

[10] I. Gryczynski, H. Malak, J. Lakowicz, R. *Biospec.* **1997**, 3, 97-101.

[11] J. R. Lakowicz, I. Gryczynsiki, H. Malak, Z. Gryczynski *Photochem. Photobiol.* **1996**, 64, 632-635.

[12] J. Palero, W. Garcia, C. Saloma *Opt. Comm.* **2002**, 211, 65–71.

[13] J. Chen, K. Midorikawa *Opt. Let.* **2004**, 29, 1354.

[14] M. O. Cambaliza , C. Saloma *Opt. Comm.* **2000**, 184, 25-35.

[15] J. R. Lakowicz, I. Gryczynski *Biophys. Chem.* **1992**, 45, 1-6.

[16] G. R. Fleming, J. M. Morris, R. J. Robbins, G. J. Woolfe, P. J. Thistlethwaite, G. W. Robinson *Proc. Natl. Acad. Sci. USA*. **1978**, 75, 4652-4656.

[17] A. N. Pisarevskii, S. N. Cherenkevich, V. T. Andrianov *Zhurnal Prikladnoi Spektroskopii*,. **1966**, 5, 621-624,.

[18] P. R. Monson, W. M. McClain *J. Chem. Phys.* **1969**, 53, 29.

[19] P. R. Monson, W. M. McClain *J. Chem. Phys.* **1971**, 56, 4817-4825.

[20] R. Niesner, B. Peker, P. Schlüsche, K.-H. Gericke *ChemPhysChem.* **2004**, 5, 1141-1149.

[21] J. R. Lakowicz, Principles of fluorescence spectroscopy Kluwer Academic/Plenum Publishers, New York, **2006**.

[22] U. Brackmann, Lambdachrome Laser dyes, Lambda Physik GmbH, Göttingen, Germany, **1986**.

[23] R. Wijnaendts van Resand, R. Vogel, S. Provencher *Rev Sci Instrum*. **1982**, 53, 1392-1397.

[24] S. Georghiou, M. Thompson, A. K. Muikhopadhyay *Biochim. Biophysic. Act.* **1982**, 688, 441-452.
[25] H. Güsten, M. Rinke, H. O. Wirth *Appl. Phys.* **1988**, 45, 279-284

6 Two-Color Two-Photon excitation of intrinsic protein fluorescence: a label free observation of a proteolytic digestion of BSA

6.1 Abstract

Two-color two-photon (2c2p) excitation fluorescence is used to monitor the enzymatic cleavage of bovine serum albumin (BSA) by subtilisin. Fluorescence is generated by irradiation with spatially and temporally overlapping femtosecond laser beams resulting in simultaneous absorption of an 800 nm and 400 nm photon. Thereby, the fluorescent amino acid tryptophan present in the BSA is excited corresponding to an effective one photon wavelength of 266 nm. The progress of the protein cleavage is monitored by time resolved fluorescence analysis. The fluorescence lifetime of tryptophan decreases during the reaction. This demonstrates a novel label free multi photon observation technique for conformational changes of proteins containing tryptophan. Due to the strong 2c2p fluorescence signal it is suitable for fast evaluation and monitoring of protein reactions. The course of the reaction was monitored simultaneously by gel electrophoresis. In contrast to conventional one photon techniques 2c2p excitation enables label free protein fluorescence studies without irradiating the sample with UV light. Due to the dependence of the excitation on the power of both laser beams excitation is limited to a relatively small focal volume. This results in dramatically reduced overall photo damage compared to direct UV irradiation. This method can be easily extended to microscopic imaging techniques.

6.2 Introduction

Fluorescence assays have become an indispensable tool for biological relevant research.[19] For that reason very sophisticated labeling techniques have been developed to match almost every requirement.[12] Additionally, a vast arsenal of differently labeled biomolecules is available ready for use. Although labeling of biomolecules offers many possibilities and advantages, it is not the undisturbed biological system that is under observation. Since the typical fluorogenic group introduced to the biomolecule is not very small, a different behavior

of the system might therefore occur. Furthermore, from a practical point of view, labeling requires an additional step of preparation which might be easy for simple biochemical reactions but can be challenging for in vivo experiments. This problem can be avoided using intrinsic fluorescence. Especially in case of proteins, staining is often not necessary, because many proteins contain fluorescent amino acids,[19] which can function as a natural fluorescence tag allowing monitoring the undisturbed biological system.

From the three fluorescence amino acids (phenylalanine, tyrosine and tryptophan) it is tryptophan which offers the highest fluorescence quantum yield of all fluorescent amino acids. [19] Consequently it is mainly used for all kinds of autofluorescence assays as well as for every day applications as protein detection on HPLC or gel electrophoresis.

The main drawback for all these applications is the fact that the absorption maximum of tryptophan (280 nm)[19] and the other fluorescent amino acids lies in the UV, where many biological compounds are sensitive to. Especially photo stress applied to DNA is not desired.[42] Hence, strong irradiation with UV light can photo damage the system under investigation. [49, 50] For microscopic applications the use of one photon excitation in the UV is additionally limited by increased scattering and conventional microscope optics having no transmission at the desired wavelengths. Two-photon techniques circumvent these problems.[2] Due to the quadratic dependence of the absorption on the excitation power the excitation is limited to the focal region, in case of a microscope objective to a very small volume.[51] This reduction of excitation volume effectively reduces the overall photo damage. However, as the two-photon absorption cross sections are extremely small, [52] very high power levels are required to achieve efficient excitation. These high power levels can only be applied to biological samples by using pulsed excitation. [53] Otherwise the introduced amount of energy would be too high. Thus, laser pulses should be as short as possible. Currently the most ideal excitation source for two-photon excitation is the Ti:Sa femtosecond laser providing ultra short laser pulses with extremely low pulse energies.[32] Unfortunately femtosecond laser sources which provide sufficient power for two-photon excitation are still limited to the red or near IR region (700nm -1000 nm) offering an effective spectral window for two-photon excitation from 350 nm to 500 nm.

One possibility to overcome this restriction in wavelength is the use of two photons of different color. Using the fundamental and second harmonic of a Ti:Sa results in a two-color, two-photon (2C2P) absorption being equivalent to an effective excitation wavelength between 233 nm and 333 nm.[11, 54] For example, two spatially and temporally overlapping laser pulses

of 400 nm and 800 nm can be used to excite tryptophan or other UV fluorophores at an effective excitation wavelength of 266 nm. Therefore, 2C2P allows highly time resolved fluorescence lifetime measurements without applying UV-light to the sample. Previously we showed experimentally that 2C2P excitation of

different chromophores (using spatially and temporally overlapping femtosecond laser pulses) is an excellent alternative to one-photon excitation and a useful extension to conventional two-photon techniques. [54]

Analogously to conventional one-color two-photon excitation, the excitation is limited to the focal region only due to the quadratic dependence on the total excitation power, or, to be more precise, to the product of the power of each color. In additional to the resulting intrinsic 3D resolution being important for microscopic application, this offers the possibility of altering the power ratio of both colors independently without changing the generated fluorescence intensity. For example, using an excess power of the 800 nm can be useful if the sample is potentially sensitive to high intensities of 400 nm. Furthermore, light at 800 nm is less scattered than at 400 nm by most biological media. Therefore, higher penetration depths can be achieved.

Along with this newly gained access to multi photon excitation of tryptophan and other UV fluorophores the 2C2P technique offers an excellent basis for time resolved fluorescence measurements like fluorescence lifetime and fluorescence anisotropy decay measurements. The introduction of femtosecond laser pulses allowed the use of all known time domain techniques like time gating or time correlated single photon counting (TCSPC) resulting in excellent time resolution.[36, 55] Furthermore, the fluorescence lifetime of tryptophan is very sensitive to its surrounding.[27, 29, 47, 56] Thus, the combination of multi photon excitation and time resolved measurement of fluorescence offers a multitude of applications monitoring protein reactions or modifications.

Fluorescence lifetime measurements present a powerful tool giving significant additional information compared to pure intensity measurements.[19, 33, 35] Measurements of fluorescence lifetimes are independent of concentration and excitation intensity. Thus, this

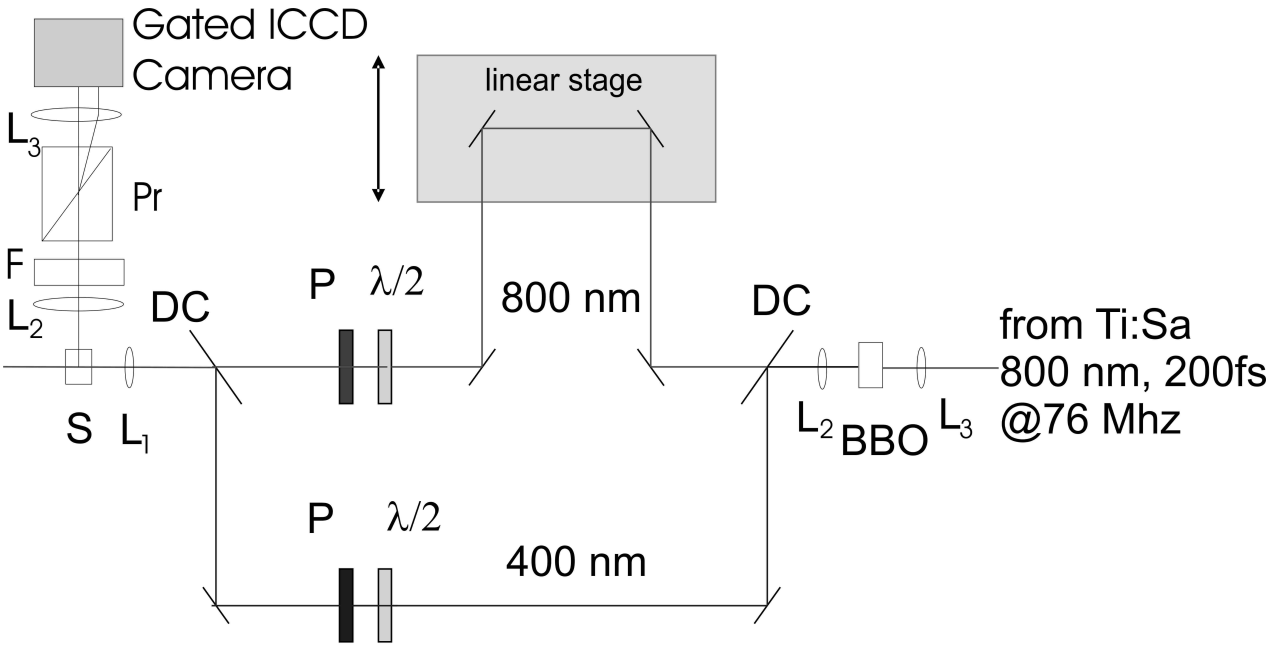

Figure 6.3: Experimental setup for 2c2p excitation fluorescence using femtosecond laser pulses. BBO = bariumborate crystal for frequency doubling, L = lens, DC =dicroic mirror, λ/2 = half wave plate, F = set of filters (Semrock NF01-405U,Semrock NF01-808U both at 10° angle and a interference filter 340/80 nm) and Pr = Rochon quarz prism, 5° deviation angle. The linear stage is used to adjust temporal overlap of the pulses in the sample.

method is relatively insensitive to uneven distribution of the fluorophore or fluctuation in laser power.

Fluorescence lifetime is strongly influenced by a large variety of different interactions between the fluorophore and its surrounding. Specifically designed fluorophores will change their fluorescence lifetime when a specific parameter of the environment changes. Therefore, highly specialized probes for all kinds of parameters have been established.[14, 15, 19, 57, 58] With the appropriate excitation source fluorescence lifetime measurements of auto fluorescence from biological samples can be used to monitor changes in the environment of the respective fluorophore. Although the fluorescence lifetime of these endogeneous fluorophores is often much more complicated to interpret, it can provide valuable information about processes inside a biological system (e.g. binding of NADPH to enzymes).[18, 44]

To the best of our knowledge, we present the first 2C2P based protein fluorescence assay. A combined application of 2C2P excitation and fluorescence lifetime measurements will be demonstrated in this article. As an example we will monitor the progress of the proteolytic cleavage of bovine serum albumin (BSA) by subtilisin.[59]

The strong fluorescence signal allows short acquisition times even with a rather simple experimental setup. A more sophisticated setup using high numerical aperture objectives will enhance the efficiency of excitation as well as the fluorescence detection allowing bioassays fast enough for high throughput screening.

6.3 Results and Discussion

We studied two-color two-photon (2c2p) excitation fluorescence of tryptophan and the protein bovine serum albumin (BSA) which contains three tryptophans. 2c2p detection of tryptophan in solutions has been studied previously using femtosecond laser pulses.[54] Here we present the first application of 2c2p excitation on intrinsic protein fluorescence.

6.3.1 Cross correlation experiment

For realization of a 2c2p excitation a temporal and spatial overlap of the femtosecond pulses is required. Figure 6.2 illustrates the data obtained from a cross correlation experiment where the delay between the two excitation laser pulses is altered using the optical delay line implemented in the optical path of the red light.

As expected 2c2p fluorescence from tryptophan occurs only when both laser pulses coincide at the same time in the sample. Lack of temporal overlap of the pulses leads to a fluorescence signal of less than 2% of the signal obtained from overlapping excitation pulses. The solid curve in Fig. 6.2 is a Gaussian distribution fitted to the experimental data using a non linear least square fit procedure. The FWHM value of the cross correlation curve is 272 fs which is in good agreement with the initial pulse width of about 200 fs.

6.3.2 2c2p excitation of intrinsic protein fluorescence

Figure 3 shows the fluorescence signal from a 0.1 mM solution of BSA in PBS. The columns labeled with “400nm + 800 nm” represent the signal upon irradiation of both colors, the columns labeled with either “400 nm” or “800 nm” represent the signal present upon irradiation with one color. The strongest fluorescence signal occurs if the 400 nm and 800 nm beam

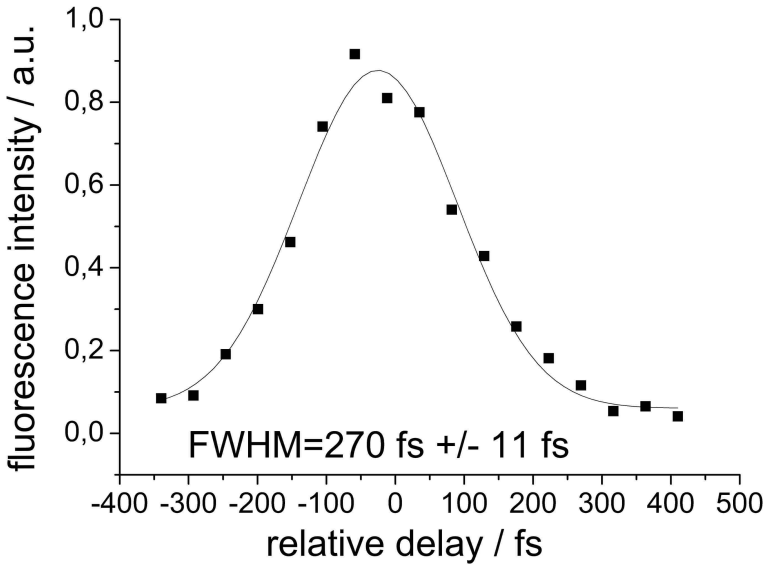

Figure 6.4: Cross correlation experiment with a 0.1 mM solution of BSA in PBS. Maximum fluorescence intensity is observed for no time delay between the pulses. With increasing delay the fluorescence intensity decreases. A Gaussian distribution is fitted to the experimental data.

coincide in the sample. As long as the product of the excitation powers of both colors remain constant a variation of the excitation power leads to a constant fluorescence signal, provided that the fluorescence signal of illumination with each color alone is subtracted from the total fluorescence. For illumination with 800 nm almost no signal can be detected for all applied power levels. Hence, no three-photon excitation is observed. Excitation at 400 nm leads to a weak fluorescence signal. The dependence of the fluorescence signal present at 400 nm irradiation exclusively is shown in Figure 6.4. This is consistent with a 1c2p excitation of

tryptophan using the strong absorption band around 200 nm in the tryptophan absorption spectrum.[19] For such a 1c2p excitation a quadratic dependence of the fluorescence signal on the excitation power is expected. The presence of such a two-photon process is confirmed by the slope in figure 4. A logarithmic plot leads

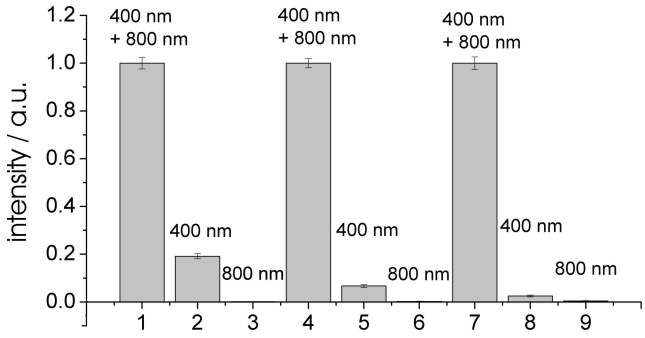

Figure 6.5: Fluorescence intensities upon irradiation of a 0.1 mM BSA solution in PBS with 400 nm and 800nm light at different power levels. Columns labeled with "400nm + 800 nm" represent the 2c2p excitation fluorescence signal which is obtained by subtracting the fluorescence signal resulting from irradiation with one color only from the total fluorescence signal. For better comparison the data are normalized to the 2c2p fluorescence signal. Error bars indicate the standard deviation of 30 measurements. Power levels: column 1-3: 800 nm : 112.5 mW, 400 nm : 8.0 mW; column 4-6: 800 nm : 225 mW, 400 nm 4 mW; column 7-9: 800 nm : 450 mW, 400 nm : 2.0 mW.

to a slope of 1.7. Albeit smaller than two, this value clearly indicates a two-photon process being the origin of the fluorescence signal. The deviation could be caused by a linear background signal or may be explained by intramolecular energy transfer out of the excited S2 state.

However, as demonstrated in figure 6.3, this background signal resulting from a 1c2p excitation at 400 nm can be almost completely suppressed by decreasing the power level at that wavelength. The second column from the right represents a background signal from 400 nm irradiation of about 2% of the 2c2p signal. The loss in 2c2p fluorescence signal is compensated by increasing the power level at 800 nm. This is possible because the fluorescence intensity is dependent on the product of the photon fluxes of both colors.

$$dN/dt = -\delta \cdot I1(800\ nm) \cdot I2(400\ nm) \cdot N$$

With N = number of molecules in the ground state, δ = two photon absorption cross section, and I = photon flux.

Hence, access intensity at 800 nm can be used while only small intensities at 400 nm light are necessary. This has a significant positive effect when using 2c2p excitation in microscopy. Near infrared light can penetrate much deeper into biological samples as it is much less scattered or absorbed as visible or UV light. This allows a high penetration depth of the imaging method and also keeps the photo damage low.

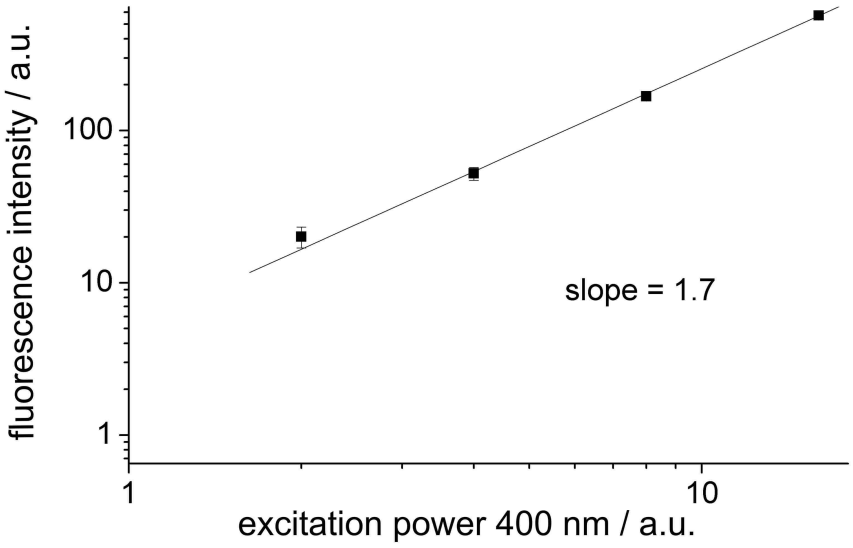

Figure 6.6: Dependence of the fluorescence signal on excitation intensity at irradtiation with 400 nm exclusively. The slope indicates a two-photon process with small linear contribution.

6.3.3 Fluorescence lifetime after 2c2p excitation

After adjustment of the excitation intensities for the optimal 2c2p excitation fluorescence signal, fluorescence lifetime measurements in the time domain are performed. The fluorescence lifetimes of tryptophan and BSA are shown in Figure 6.5. The lifetime value for tryptophan resulting from a monoexponential fit of 2.5 ns is consistent with observations from Fleming et al. for a one photon excitation.[27] Monoexponential fit of the fluorescence intensity decay of BSA rendered a fluorescence lifetime of 6.1 ns which, again, agrees with

fluorescence lifetime measurements performed using one-photon and 1c2p excitation.[60] Consequently we can conclude that the fluorescence occurs out of the same excited stated, i.e. the S1.

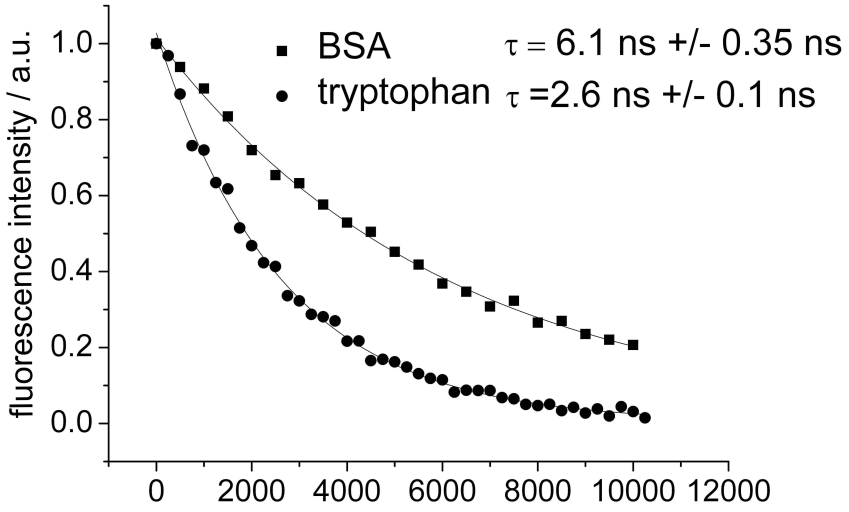

Figure 6.7: Fluorescence lifetimes of 0.1 mM solution of tryptophan and BSA, respectively, in PBS. Mono exponential fitting renders (mean) fluorescence lifetimes of 2.6 ns for tryptophan and 6.1 ns for BSA.

6.3.4 Label free monitoring of a protein digestion

A proteolytic digestion of BSA by the hydrolase subtilisin is monitored by means of fluorescence lifetimes after 2c2p excitation of intrinsic fluorescence of BSA. It was found that degradation of BSA into smaller fragments using the protease subtilisin leads to a significant change in fluorescence lifetime. Figure 6.6 shows the decay of fluorescence intensity at arbitrarily selected times of the enzymatic reaction. The data of figure 6.6 A were obtained using a 1mM solution of BSA in PBS while the data of figure 6.6 B were obtained from measurement of a 0.1 mM solution of BSA in PBS. To each protein solution subtilisin was added (0.01 mM).

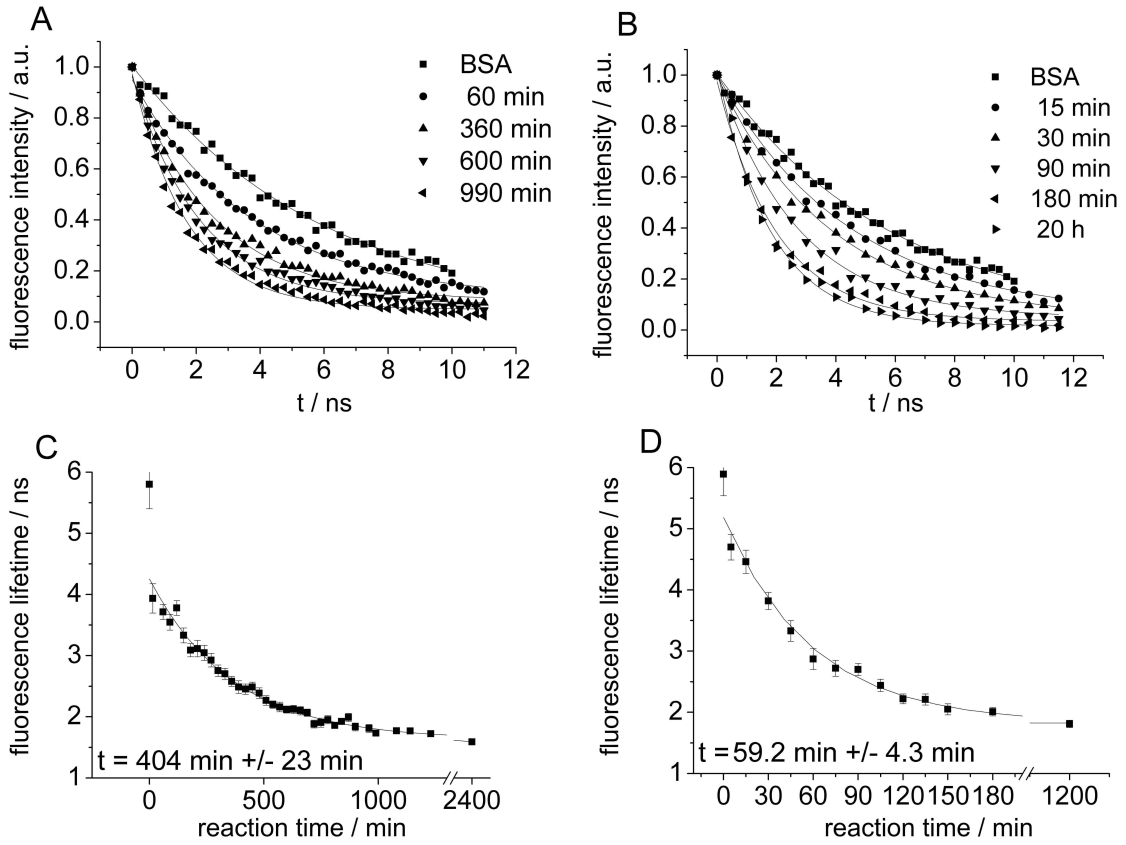

Figure 6.6: A and B represent selected fluorescence decays at different times of the reaction. A represents data from a 1 mM BSA solution in PBS while B represents data from a 0.1 mM BSA solution in PBS. To either solution ~ 0.01 mM subtilisin was added. Solid lines represent mono exponential fitting for determination of the fluorescence lifetime. The diagrams below (C and D) show the obtained fluorescence lifetimes plotted versus the reaction time. After a rapid decay of the fluorescence lifetime during the first reaction period, a mono exponential decay fits the data best.

Although subtilisin contains also tryptophan, a 0.01 mM enzyme solution without BSA gave a fluorescence intensity of only 6 % of the intensities obtained at the beginning of the observation of the 0.1 mM BSA enzyme reaction. A mono exponential decay was found to be the overall best fit for the intensity decay data. The obtained fluorescence lifetime decreases with increasing reaction time. Shortly after the start of the enzymatic reaction, the fluorescence lifetime drops from its initial value of about 6 ns to 4.5 ns. With the ongoing cleavage the lifetime decreases further before it settles at a final value below 2 ns. The decay of fluorescence lifetime during the reaction is illustrated by the lifetime versus reaction time plots shown in figures 6.6 C and 6.6 D. After the initial fast drop in lifetime, a mono exponentially fit describes the data well. For the reaction with the higher BSA concentration a decay constant of 404 min +/- 23 min was obtained. For the lower concentration a value of 59 min +/- 4 min was found.

The correlation of the fluorescence lifetime with the gel electrophoresis shown in figure 6.6 leads to the conclusion that the fluorescence lifetime of the intrinsic protein fluorescence decreases with decreasing fragment size. This is somewhat surprising since it is known that the fluorescence lifetime of tryptophan is dependent on the conformation of the protein in a very complicated way and it eventually depends also on the conformation of tryptophan itself.[21, 29] The rotational conformations of tryptophan itself as well as the quenching abilities of its neighborhood have in most cases a far bigger effect on its lifetime than the overall size or weight of the protein. Hence, it can be concluded that in BSA the tryptophan residues are in a conformational state where the rate constants for quenching processes are rather slow. The quenching rate obviously increases when the fragments become smaller, resulting in a reduced fluorescence lifetime.

It is noteworthy that the final fluorescence lifetime settles below the fluorescence lifetime of the free tryptophan. This is consistent with the experiments performed by Fleming et. al.[27] who measured a fluorescence lifetime for a dipeptide of tryptophan of about 1.5 ns. Hence, the measured lifetime indicates that at the end of the reaction polypeptides are still present. If the proteolytic cleavage proceeded to a stage of isolated amino acids a longer fluorescence lifetime around 2.5 ns is expected.

The data presented in Figure 6.6 demonstrate the possibility of a label free monitoring of the proteolytic cleavage of BSA by subtilisin by means of fluorescence lifetime measurements of the intrinsic protein fluorescence. First of all it is a surprising observation that a mono exponential decay is the best fit to the intensity decay. The fluorescence of a single tryptophan protein like human serum albumin is usually described as a bi- or even triexponential decay.[20] Compared with the results from the gel electrophoresis it can be assumed that the measured intensity decays represent a superposition of a relative broad distribution of different lifetimes arising from a broad distribution of protein fragments with different molecular weights and conformations. Nevertheless, applying a stretched exponential to the data does not improve the fit.[61]

6.3.5 Fluorescence anisotropy

In order to ensure that the measurements of the fluorescence lifetime are not significantly influenced by anisotropic effects, the fluorescence anisotropy decay of BSA was measured.

Probably due to internal energy transfer the tryptophan fluorescence in BSA exhibits a very small initial fluorescence anisotropy of 0.07. This very low anisotropy does not allow a determination of the rotational diffusion constant with an acceptable accuracy. Hence, the rotational diffusion which should decrease with the size of the protein fragments cannot be measured with sufficient accuracy. However, it clearly demonstrates that the fluorescence lifetime measurements are not disturbed by anisotropic effects.

6.3.6 Gel electrophoresis

The fluorescence decay measurements of the proteolytic cleavage of BSA were complemented by monitoring the reaction by gel electrophoresis. Figure 6.7 shows the gel for the measurements of a 1 mM BSA solution in PBS corresponding to the fluorescence data presented in figure 6.6 A and below. The photographs of the electrophoresis gels show the expected increasing occurrence of smaller protein fragments. 15 min after the start of enzymatic reaction (see figure 6.7) no BSA is observed. Three strong bands indicating molecular weights around 30 kDa and some distinct bands around 20 kDa, 15 kDa and 5 kDa can be seen. One of the three bands around 30 kDa can be correlated with subtilisin (~ 27 kDa). During the following ten measurements the distribution of fragments broadens to give fragments with molecular weights of up to 30 kDa. After 3 hours an almost even distribution is observed. During the following measurements a tendency to smaller fragments can be seen. After 5 hours of reaction the gel shows a shift to smaller fragments well below 6 kDa. After 9 hours the majority of protein fragments have a molecular weight smaller than 6 kDa as a result of the hydrolytic cleavage of the protein. Due to this light weight they run out of the gel and cannot be detected anymore (gels not shown).

For practical use, e.g. molecular screening applications a correlation between molecular weight, reaction time and fluorescence lifetime would be desired. In addition to figures 6 C and D figure 6.8 shows a correlation between molecular weight and reaction time. The intensities of the 30 kDa, 20 kDa and the 6 kDa band of the gel shown in figure 6.7 are analyzed over the first 500 minutes of the reaction shown in figures 6 A and C.

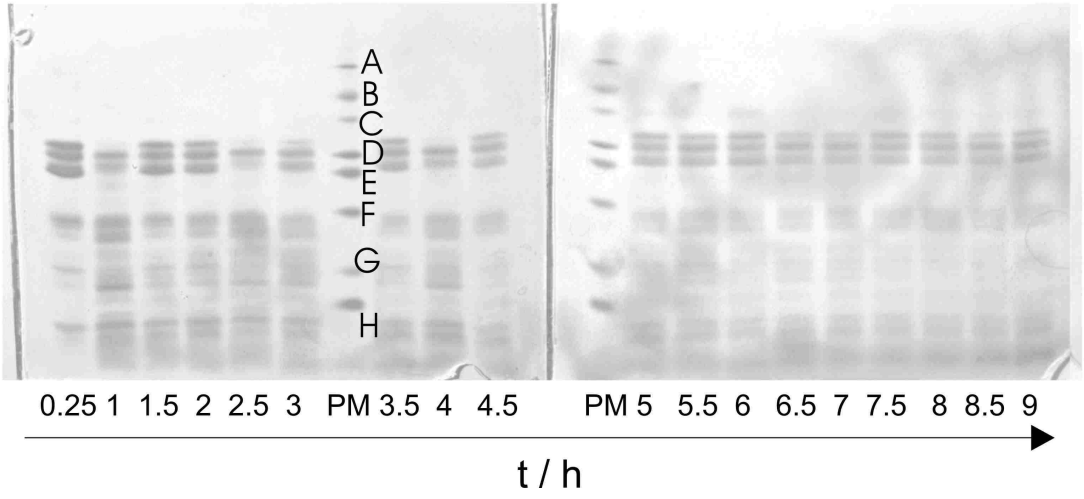

Figure 7: Gel electrophoresis of the reaction mixtures of the 1 mM BSA digestion by subtilisin quenched at different times of reaction. Molecular weight of the protein marker (PM) proteins: (A) 66 kD, (B) 45 kD, (C) 36 kD, (D) 29 kD, (E) 24 kD, (F) 20.1 kD, (G) 14.2 kD, (H) 6.5 kD.

This is achieved by using a horizontal intensity read out of the first two gel images following the respective band employing simple photo software. The data were corrected with respect to the background between two adjacent bands.

This intensity data of the three bands were plotted versus the reaction time to form figure 6.8. A cubic polynomial least square fit to the data has been added for visional convenience.

Figure 6.8 gives a good impression of the origin of the decreasing fluorescence lifetime as well as a hint indicating how a calibration fluorescence lifetime towards molecular weight distribution can be achieved. It can be seen that the intensity of the 30 kDa band decreases rapidly while the intensity of 20 kDa band remains constant during the first measurements or even increases before it decreases much slower than the 30 kDa band. Although containing more

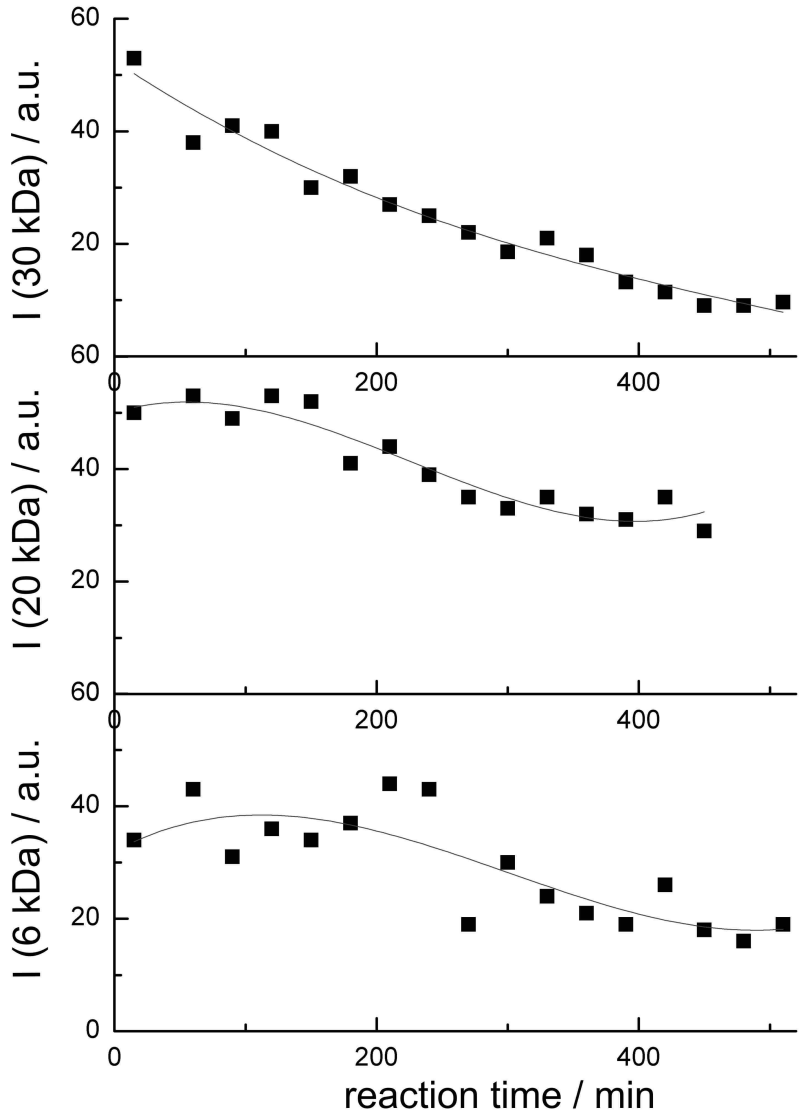

Figure 8: Intensity of the 30 kDa, 20 kDa and 6 kDa band of the electrophoresis gel as a function of the fluorescence lifetime of the reaction mixture. The solid line represents a cubic polynomial fit to the data serves as a guide to the eye. The data represents measurement performed during the first 500 min of the reaction and corresponds to the data shown in figure 6 A and C and figure 7.

noise, the 6 kDa band shows a similar yet even more pronounced behavior than the 20 kDa band.

As the evanescence of the 30 kDa band is much faster than those of the smaller fragments it can be seen that the distribution shifts to smaller fragments during the reaction, which then dominate the fluorescence lifetime. Furthermore, the fits to the data do also imply the

expected built-up in the concentration of the smaller fragments at the beginning of the reaction. Hence, a carefully performed gel electrophoresis with high resolution and subsequent intensity read out of each band over time can provide calibration data for correlation of the fluorescence lifetime of tryptophan with a molecular weight distribution.

6.4 Conclusion

We present a label free observation method for a proteolytic digestion using two-color two-photon excited intrinsic fluorescence of the involved protein. 2c2p using femtosecond laser pulses gives us a multi photon technique at hand providing low photo damage, superior temporal resolution, intrinsic 3D resolution and a potentially high penetration depth. Additionally, 2c2p represents a convenient technique for extension of the effective wavelength range of the Ti:Sa femtosecond laser. In addition to the spectral windows for one photon (700 nm -1000 nm) and conventional one-color two-photon techniques (350 nm - 500 nm) effective excitation from 233 nm – 333 nm can be achieved.

Changes in fluorescence lifetime of tryptophan depending on its environment have been reported earlier. [56, 62] Additionally, numerous fluorescence assays have been published where a shift in the fluorescence spectrum of tryptophan is observed upon a change in tryptophan surrounding.[22, 63, 64] These shifts also go hand in hand with a change in fluorescence lifetime.[65] Therefore, the observation of the digestion of tryptophan via fluorescence lifetime is just one first example demonstrating the power of a time resolved 2c2p setup using femtosecond laser pulses from a Ti:Sa applied to the observation of protein reactions. This can be applied for a variety of different assays using intrinsic protein fluorescence.[39-41]

Moreover, the presence of a multi-photon process for excitation makes this method ideal for microscopic applications where the use of high numerical aperture microscope objectives allows reducing the laser power to a minimum. Due to the quadratic dependence of the excitation on the total excitation power excitation is confined to a small focal volume. Hence, 2c2p microscopy possesses intrinsic 3D resolution combined with dramatically reduced photo damage compared to conventional one photon techniques. The wavelengths of 400 nm and 800 nm are considerably less harmful to biological samples than the corresponding 266 nm in case of a one photon excitation. A large excess of 800 nm light can be used allowing minimization of the 400 nm power level. Hence, UV intrinsic fluorophores can be excited

without the irradiation of UV light. With respect to 3 photon excitation the absolute power level can be kept comparatively small because the two-photon absorption cross sections are much larger than the three photon ones.[66] With the help of femtosecond laser pulses this technique provides an ideal basis for time resolved time domain measurements with temporal resolution of only a few ps. Since the main excitation power is provided by the 800 nm beam, a high penetration depth into biological samples can be expected, because near IR is less scattered and absorbed in biological tissue than shorter wavelengths.[31] Due to the dependence of the excitation probability on the product of the intensities of both excitation colors it is this less scattered and highly intense IR focus that determines the resolution in deep tissue imaging. Application of this new 2c2p fluorescence microscopic technique will offer many new opportunities for which the discussed label free observation of a protein digestion is just one example.

6.5 Experimental Section

The experimental setup is shown in figure 6.1. Femtosecond laser pulses from a NdYVO4 pumped Ti:Sa (mira 900 B, Coherent) are frequency doubled using a beta-bariumborate (BBO) crystal. The second harmonic (400 nm) and the remaining fundamental (800 nm) are separated by a dichroic mirror. A linear stage is implemented ensuring exact temporal overlap of the laser pulses in the sample. The excitation power is adjusted by a set of lambda half plate and thin layer polarizer. After reunion of both beams via a second dichroic mirror they are focused into the sample via an achromatic lens with a focal length of 5 cm. Spatial overlap can be adjusted by replacing the cuvette with a pin hole. Temporal overlap is adjusted using a highly efficient 2c2p fluorescent dye, e.g. p-terphenyl (PTP) in cyclohexane. 2c2p excitation is only present at spatial and temporal overlap of the excitation pulses of each color (figure 2). The fluorescence is collected by a lens (L2) with 25 mm focal length and a diameter of 30 mm. Optionally, after passing a set of filters (Semrock NF01-405U,Semrock NF01-808U both at 10° angle and a interference filter 340/80 nm), the fluorescence can be analyzed in terms of polarization using a Rochon prism. Finally the fluorescence is projected onto a time gated ICCD camera system (picostar, LaVision GmbH, Göttingen). The adjustable gate width, 200 ps to 1 ns, in combination with a delay generator (Kentech Instruments Ltd.) allows a temporal resolution of about 10 ps.

BSA, subtilisin was purchased from Sigma-Aldrich and used without purification. A 1 mM and 0.1 mM solution of BSA are prepared using PBS buffer. Subtilisin is added to the protein solution giving concentration of about 0.01 mM.

Gel electrophoresis is performed using polyacrylamide support matrices under discontinuous denatured conditions (125 V, 2 h) after quenching the enzymatic reaction by heat. As a ruler for molecular weight the protein marker M3913 from Sigma-Aldrich is used. Staining reagent was Coomassie Blue.

6.6 Acknowledgements

Financial support by the DFG (Deutsche Forschungsgemeinschaft) under grant no. Ge496/20 is gratefully acknowledged.

6.7 References

[1] H. Shuman, J. M. Murray, C. DiLullo *Biotechniques*. **1989**, 7, 154-163.

[2] W. Denk, J. H. Strickler, W. W. Webb *Science, New Series*. **1990**, 248, 73-76.

[3] F. Helmchen, W. Denk *Nautre Methods*. **2005**, 2, 933-940.

[4] R. Heintzmann, P. A. Benedetti *Appl. Opt.* **2006**, 45, 5037-5045.

[5] D. Karadaglić, T. Wilson *Micron*. **2008**, 39, 808-818.

[6] K. I. Willig, R. R. Kellner, R. Medda, B. Hein, S. Jakobs, H. S. W. *Nature Methods*. **2006**, 3, 721-723.

[7] B. R. Rankin, R. R. Kellner, S. W. Hell *Opt. Lett.* **2008**, 33, 2491-2493.

[8] A. Egner, C. Geisler, C. v. Middendorff, H. Bock, D. Wenzel, R. Medda, M. Andresen, A. C. Stiel, S. Jakobs, C. Eggeling, A. Schönle, S. W. Hell *Biophys. J.* **2007**, 93, 3285-3290.

[9] R. Heintzmann, G. Ficz *Brief Funct Genomic Proteomic*. **2006**, 5, 289-301.

[10] P. R. Monson, W. M. McClain *J. Chem. Phys.* **1971**, 56, 4817-4825.

[11] J. R. Lakowicz, I. Gryczynsiki, H. Malak, Z. Gryczynski *Photochem. Photobiol.* **1996**, 64, 632-635.

[12] K. M. Marks, G. P. Nolan *Nature Methods*. **2006**, 3.

[13] R. Y. Tsien *Biochemistry*. **1980**, 19, 2396-2404.

[14] P. H. Hai-Jui Lin, Jung Sook Kang, Joseph R. Lakowicz. **2001**.

[15] H. S. Hai-Jui Lin, Joseph R. Lakowicz *Analytical Biochemistry*. **1999**, 269, 162-167.

[16] R. Y. Tsien *Annu Rev Biochem*. **1998**, 67, 509-544.

[17] J. M. Tavare, L. M. Fletcher, P. B. Oatey, L. Tyas, J. G. Wakefield, G. I. Welsh *Diabetic Medicine*. **2001**, 18, 253-260.

[18] A. A. H. Shaohui Huang, Watt W. Webb *Biophysical Journal*. **2002**, 82, 2811–2825.

[19] J. R. Lakowicz, Principles of fluorescence spectroscopy Kluwer Academic/Plenum Publishers, New York, **2006**.

[20] J. R. Lakowicz, I. Gryczynski *Biophys. Chem.* **1992**, 45, 1-6.

[21] M. Hellings, M. De Maeyer, S. Verheyden, Q. H. Els, J. M. Van Damme, W. J. Peumans, Y. Engelborghs *Biophys. J.* **2003**, 85, 1894-1902.

[22] A. V. Ostrovsky, L. P. Kalinichenko, V. I. Emelyanenko, A. V. Klimanov, E. A. Permyakov *Biophys. Chem.* **1987**, 30, 105-112.

[23] Y. Engelborghs *Journal of Fluorescence*. **2003**, 13, 9-16.

[24] M. K. Kuimova, G. Yahioglu, J. A. Levitt, K. Suhling *J Am Chem Soc*. **2008**, 130, 6672-6673.

[25] R. Niesner, B. Peker, P. Schlüsche, K. H. Gericke, C. Hoffmann, D. Hahne, C. Müller-Goymann *Pham Res*. **2005**, 22, 1079-1087.

[26] R. K. Benninger, Y. Koç, O. Hofmann, J. Requejo-Isidro, M. A. Neil, P. M. French, A. J. DeMello *Anal. Chem.* **2006**, 78, 2272-2278.

[27] G. R. Fleming, J. M. Morris, R. J. Robbins, G. J. Woolfe, P. J. Thistlethwaite, G. W. Robinson *Proc. Natl. Acad. Sci. USA*. **1978**, 75, 4652-4656.

[28] N. Vekshin, M. Vincent, J. Gallay *Chem. Phys. Let.* **1992**, 199, 459-464.

[29] Y. Engelborghs *Spectrochimica Acta*. **2001**, 57, 2255-2270.

[30] R. Niesner, V. Andresen, J. Neuman, H. Spieker, M. Gunzer *Biophys. J.* **2007**, 93, 2519-2529.

[31] R. Weissleder, V. Ntziachristos *Nature Medicine*. **2003**, 9, 123-128.

[32] R. Niesner, W. Roth, K.-H. Gericke *Chem. Phys. Chem.* **2004**, 5, 678-687.

[33] D. Elson, J. Requejo-Isidro, I. Munro, F. Reavell, J. Siegel, K. Suhling, P. Tadrous, R. Benninger, P. Lanigan, J. McGinty, C. Talbot, B. Treanor, S. Webb, A. Sandison, A. Wallace, D. Davis, J. Lever, M. Neil, D. Phillips, G. Stamp, P. French *Photochem. Photobiol. Sci.* **2004**, 3, 795-801.

[34] W. Becker, A. Bergmann, G. Biscotti, A. Rück *Proc. Spie.* **2004**, 5340, 1-9.

[35] E. Gratton, S. Breusegem, J. Sutin, Q. Ruan, N. Barry *Biomed. Opt.* **2003**, 8, 381-390.

[36] K. Suhling, P. M. W. French, D. Phillips *Photochem. Photobiol. Sci.* **2005**, 4, 13-22.

[37] W. M. McClain *J. Chem. Phys.* **1972**, 58, 324-326.

[38] I. Gryczynski, H. Malak, J. Lakowicz, R. *Biospec.* **1997**, 3, 97-101.

[39] J. Palero, W. Garcia, C. Saloma *Opt. Comm.* **2002**, 211, 65–71.

[40] J. Chen, K. Midorikawa *Opt. Let.* **2004**, 29, 1354.

[41] M. O. Cambaliza , C. Saloma *Opt. Comm.* **2000**, 184, 25-35.

[42] A. N. Pisarevskii, S. N. Cherenkevich, V. T. Andrianov *Zhurnal Prikladnoi Spektroskopii,*. **1966**, 5, 621-624,.

[43] P. R. Monson, W. M. McClain *J. Chem. Phys.* **1969**, 53, 29.

[44] R. Niesner, B. Peker, P. Schlüsche, K.-H. Gericke *ChemPhysChem.* **2004**, 5, 1141-1149.

[45] U. Brackmann, Lambdachrome Laser dyes, Lambda Physik GmbH, Göttingen, Germany, **1986**.

[46] R. Wijnaendts van Resand, R. Vogel, S. Provencher *Rev Sci Instrum*. **1982**, 53, 1392-1397.

[47] S. Georghiou, M. Thompson, A. K. Muikhopadhyay *Biochim. Biophysic. Act.* **1982**, 688, 441-452.

[48] H. Güsten, M. Rinke, H. O. Wirth *Appl. Phys.* **1988**, 45, 279-284

[49] L.-O. Essen *BIOspektrum*. **2006**, 12, 356.

[50] R. P. Sinha, D.-P. Häder *Photochem. Photobiol. Sci.*,. **2002**, 1, 225-236.

[51] R. M. Wiliams, D. W. Piston, W. W. Webb *FASEB J*. **1994**, 8, 804-813.

[52] C. Xu, W. Zipfel *Proc. Natl. Acad. Sci. USA, Biophysics*. **1996**, 93, 10763-10768.

[53] S. M. Potter *Curr. Biol.* **1996**, 6, 1595-1598.

[54] S. Quentmeier, S. Denicke, J.-E. Ehlers, R. A. Niesner, K.-H. Gericke *J. Phys. Chem. B.* **2008**, 112, 5768-5773.

[55] A. B. Wolfgang Becker, C. Biskup, L. Kelbauskas, T. Zimmer, N. Klöcker, K. Benndorf *Proc. Spie.* **2003**, 4963, 1-10.

[56] N. Joshi, V. O. de Joshi, S. Contreras, H. Gil, H. Medina, A. Siemiarczuk *SPIE*. **1999**, 3602, 124-131.

[57] A. V. Agronskaia, H. C. Gerritsen, L. Tertoolen *Journal of Biomedical Optics*. **2004**, 9, 1230-1337.

[58] R. K. P. Benninger, O. Hofman, J. McGinty, J. Requejo-Isidro, I. Munro, M. A. A. Neil, A. J. de Mello, P. M. W. French *Optics Express*. **2005**, 13, 6275-6285.

[59] C. C. Quentmeier, A. Wehling, P. J. Walla *Journal of Biomolecular Screening*. **2007**, 12, 2-10.

[60] E. L. Gelamo, M. Tabk *Spectrochimica Acta*. **2000**, 56, 2255-2271.

[61] J. Siegel, K. C. Benny Lee, A. Vlandas, G. L. Gambaruto, S. E. D. Webb, S. Lévêque-Fort, D. S. Elson, P. J. Tadrous, G. W. H. Stamp, A. L. Wallace, M. J. Lever, P. M. W. French. **2002**.

[62] A. Siemiarczuk, C. E. Petersen, C.-E. Ha, J. Yang, N. V. Bhagavan *Cell Biochemistry and Biophysics*. **2004**, 40, 115-122.

[63] M. J. Kronman *Biochimica et Biophysica Acta*. **1967**, 19, 19-35.

[64] G. Sanyal, L. M. Richard, K. L. Carraway, D. Puett *Biochemistry*. **1988**, 27, 6229-6236.

[65] S. J. Strickler, R. A. Berg *J. Chem. Phys.* **1962**, 37, 814-822.

[66] W. R. Zipfel, R. M. Wiliams, R. Christie, A. Y. Nikitin, B. Hyman, W. W. Webb *PNAS*. **2003**, 100, 7075-7080.

7 Two-Color Two-Photon Fluorescence Laser Scanning Microscopy

7.1 Abstract

We present the first realization of a Two-Color Two-Photon Laser-Scanning Microscope (2c2pLSM) and UV fluorescence images of cells acquired with this technique. Fluorescence is excited by two-color two-photon absorption using the fundamental and the second harmonic of a Ti:Sa femtosecond laser. Simultaneous absorption of an 800 nm photon and a 400 nm photon corresponds energetically to a one-photon absorption at 266 nm. This technique for Laser-Scanning Microscopy extends the excitation wavelength range of a Ti:Sa powered fluorescence microscope to the UV. In addition to the known advantages of multi-photon microscopy like intrinsic 3D resolution, reduced photo damage and high penetration depth 2c2pLSM offers the possibility of using standard high numeric aperture objectives for UV fluorescence imaging. The effective excitation wavelength of 266 nm corresponds especially well to the excitation spectrum of tryptophan. Hence, it is an ideal tool for label free fluorescence studies and imaging of intrinsic protein fluorescence which originates mainly from tryptophan. Thus a very sensitive natural lifetime probe can be used for monitoring protein reactions or changes in conformation. First measurements reveal differences in UV fluorescence lifetimes between nucleus and cytoplasm of living MIN-6 cells. Another example for the significance of this method it was used for monitoring the binding of biotin to avidin.

7.2 Introduction

In the field of fluorescence microscopy two-photon microscopy (2PM) has become an indispensable tool over the last years. [3] Its sharp and high contrast pictures combined with its intrinsic 3D resolution and a superior penetration depth into biological tissue make it the technique of choice for many applications. Especially in the growing field of medical applications of fluorescence microscopy it is the reduced photo toxicity and high penetration depth that makes it the favorable technique. [67-69]

But even though it is used in a huge variety of different applications it is still limited to a rather small spectral window. This limitation comes from the necessity for excitation with extremely short laser pulses. Today, the light source of choice for 2PM is still the Ti:Sa femtosecond laser providing an output of about 700 nm to 1000 nm. Hence, the effective two-photon excitation is limited to a wavelengths range of 350 nm to 500 nm. In principle, an additional spectral window can be reached by using three-photon excitation.[66] However, due to extremely small three-photon absorption cross sections power levels have to be used that in most cases do not suit biological samples.

One way to overcome these limitations is to extend two-photon excitation to two-color two-photon (2c2p) excitation. [54] Basic experiments and theoretical considerations towards two-color two-photon laser scanning microscopy (2c2pLSM) have been published earlier.[11, 38, 40, 41, 70-72] We demonstrate the practicability of two-color two-photon laser scanning microscopy in an experimental setup using fundamental output of a Ti:Sa at 800 nm and the second harmonic at 400 nm. By spatially and temporarily overlapping these beams a two-color two-photon absorption with an effective excitation wavelength of 266 nm can be achieved. Hence, with 2c2pLSM the excitation range of the microscope is extended to the UV, i.e. 230 nm – 330 nm.

This spectral window is of special interest for life science, because it corresponds well with the absorption spectrum of tryptophan. Tryptophan is the amino acid which is responsible for the majority of intrinsic protein fluorescence.[19] This does not only allow label free protein detection but also monitoring of protein reactions and conformational changes in proteins. This is possible because tryptophan represents a natural built in probe whose fluorescence lifetime is sensitive chemical or conformational changes in its environment.[29, 73]

The most obvious way to excite tryptophan is of course a one-photon excitation using 280 nm light. However, using this wavelength for excitation in confocal or wide field fluorescence microscopy creates numerous problems. First of all, UV light is toxic to living cells, especially because DNA does absorb at this wavelengths, too.[50] Secondly, the shorter the wavelength becomes the more scattering in turbid media occurs resulting in dramatically reduced spatial resolution.[74] And last, such wavelengths require special optics which are not available nowadays. None of the high numeric aperture objectives ideally used for fluorescence microscopy can be used as they are not transparent for wavelengths shorter than 300 nm. Special UV objectives are available, but only with poor numerical apertures. Hence, they offer only low photon efficiency and low resolution.

2c2pLSM can be an answer to these problems. [11, 41] Using 800 nm and 400 nm for excitation of intrinsic protein fluorescence limits the excitation and hence, the absorption and photo damage to the focal region as known from other multi photon techniques. Thus, compared to one-photon excitation where excitation occurs in a vast volume of the sample multi-photon techniques reduce the photo damage by exciting only where fluorescence is desired for detection. Furthermore, the employment of longer wavelengths reduces scattering.

Using 800 nm and 400 nm light for excitation conventional high numeric objectives can be used for 2c2pLSM providing the best basis for a high resolution. Due to the Stokes shift the fluorescence occurs at wavelengths longer than 300 nm where the transmition efficiency is significantly higher.

The high penetration abilities of the 800 nm light apply as in conventional 2PM keeping the photo damage low and the resolution high. This is possible because the 2c2p absorption probability is dependent on the product of the powers of each color. This allows increasing the excitation power at 800 nm light and accordingly reducing the power at 400 nm without loss of signal. Thus, the increased scattering and photo toxicity of the 400 nm light is of minor importance since only very low powers of it are required in the focus. The resolution is prevailingly determined by the focus of the 800 nm light and its superior focusing properties in turbid media. [75]

Using a non-descanned detection in combination with sample scanning we present first 2c2pLSM-fluorescence images of MIN 6 cells demonstrating the applicability of this method for UV-fluorophore imaging inside living cells. Additionally, the application of 2c2pLSM for

monitoring the binding of biotin to avidin is demonstrated using a time gated camera combined with galvo-optic beam scanning.

7.3 Experimental setup

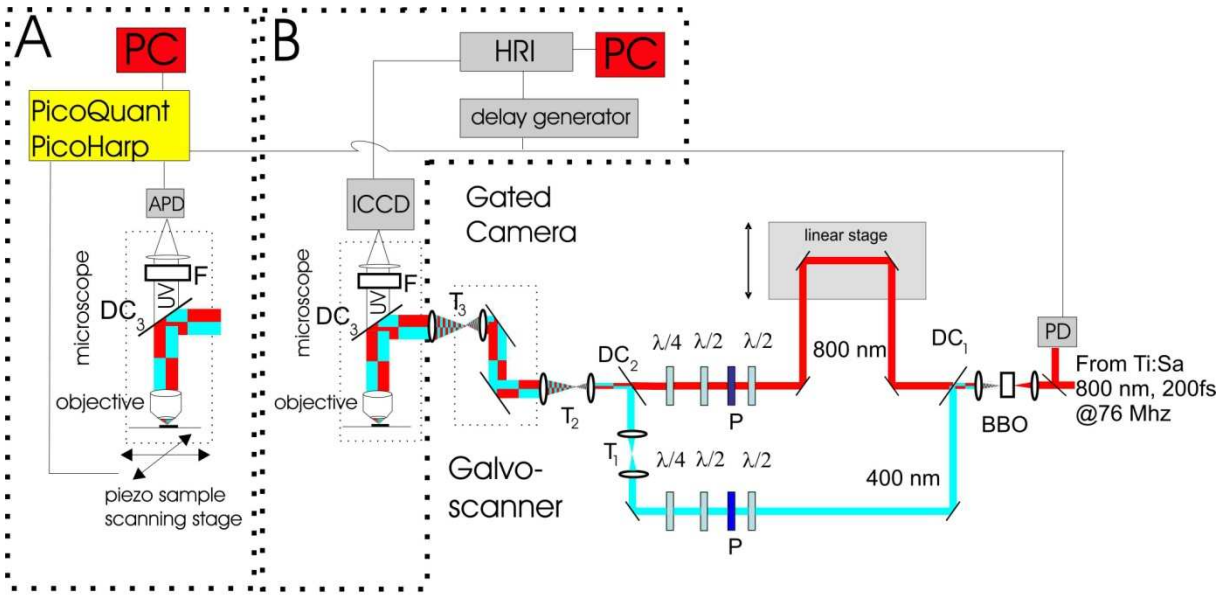

Figure 8: Experimental Setup of a 2c2pLSM using either the setup A or B. A represents the setup with avalanche photo diodes (APD) and TCSPC detection and sample scanning while B shows the setup with time gated camera system and beam scanning. With PD = photo diode, BBO= beta-bariumborate crystal; DC = dichroic mirror; λ/2 = half wave plate; λ/4 = quarter wave plate; P = polarizer; F = set of filters: interference filter 350/40 nm, notch filter 405 nm; ICCD = intensified charge coupled device, APD = avalanche photo diode, TCSPC = time correlated single photon counting.

Two different schemes of the experimental 2c2pLSM setup are shown in figure 1. In B the initial experimental setup is shown featuring a beam scanning setup with a time gated intensified charge coupled device (ICCD) camera. To enhance photon efficiency and spatial resolution we switched to a non-descanned sample scanning setup with time correlated single photon counting (TCSPC) detection (figure 1 A). The basic setup in front of the microscope is the same for both setups.

The fundamental of a NdYVO4 laser pumped Ti:Sa laser at 800 nm is frequency doubled by a beta-bariumborate (BBO) crystal as shown in figure 1. The remaining 800 nm light and the frequency doubled light are first separated by a dichroic mirror (DC1) and reunified in the same way later (DC2). Along their separated light paths the power and polarization can be

adjusted. Additionally, the optical path length of the 800 nm beam can be adjusted to match that of the 400 nm beam by an optical delay line consisting of two mirrors mounted on a motorized linear stage, ensuring temporal overlap of both laser pulses in the focal volume of the objective. Furthermore, the blue light path contains a telescope (T1) which can be adjusted to account for chromatic aberrations relative to the 800 nm light in the subsequent optical pathway. After reunion both colors pass a telescope (T2) for the purpose of beam expansion. The center of the galvo scanner is then projected by a third telescope (T3) via a dichroic mirror DC3 onto the back aperture of the objective (Zeiss plan-Neofluar 40x/1,3 oil) to ensure optimal scanning process in case of beam scanning (fig. 1 B) using a galvo scanner (GSI Lumonics).

Fluorescence is collected by the same objective and transmitted by the dichcroic mirroc DC3. After further isolation of the fluorescence by a set of filters F, the fluorescence image is projected by a quartz lens onto the photo cathode of a time gated ICCD camera system (LaVision GmbH, Göttingen, picostar). Alternatively, (fig 1 A) the camera system can be exchanged by an avalanche photo diode (APD) (micro photonic devices, Bolzano, PDM series) in combination with a TCSPC system (PicoQuant, PicoHarp 300. Scanning is then achieved using a piezo sample scanner (Physik Instrumente GmbH Karlsruhe, P-733.2CL) The galvo mirrors are then set to a defined zero position.

For initial alignment of the two laser beams the camera detection shown in scheme of B figure 1 B is used. Therefore, both laser beams are coupled into the microscope and focused through the objective into a solution of p-terphenyl (PTP) in cyclohexane. At elevated laser power fluorescence can be detected from both foci. Previous investigations showed that this fluorescence originates from a one-color two-photon excitation in case of the 400 nm beam and from a three-photon excitation in case of the 800 nm beam.[54] The fluorescence wavelength is around 350 nm. After spatial overlap is ensured temporal overlap is achieved by adjusting the optical path length of the 800 nm beam with the linear stage. Temporal and spatial overlap results in strongly increased fluorescence signal originating from the focus of the two aligned laser beams. Finally, the power of both beams can be reduced to a level, where only minor one-color two-photon excitation and almost no three-photon excitation occurs. Due to the quadratic and cubic power dependence of these excitations they decrease stronger than the 2c2p signal which is only linearly dependent on the power of each beam. Hence, 1c2p excitation with 400 nm light has a negligible contribution to the 2c2p image.

MIN 6 cells are grown cultivated in DMEM high glucose (4,5 g/L) (PAA laboratory GmbH) under carbogene atmosphere. Avidin and biotin are purchased from Sigma-Aldrich and used without further purification.

7.4 Results

Using the camera setup (figure 1B) a cross correlation experiment is performed demonstrating that the total fluorescence measured originates from a 2c2p excitation. The delay of the red beam is successively varied by moving the linear stage. Figure 2 presents the resulting data. The solid line represents a Gaussian function fitting the data best with a full width at half maximum (FWHM) of 545 fs.

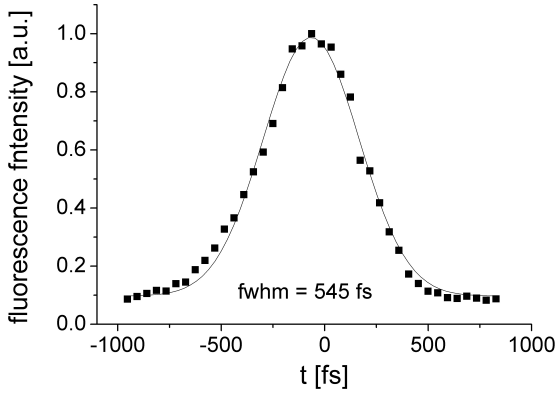

Figure 9: Cross correlation experiment where the 800 nm pulse was delayed with respect to the 400 nm beam. The solid curve represents a gaussian function fitting the data best.

Strong fluorescence is only present when both laser pulses temporally overlap in the focal volume. Each color alone gives only a weak fluorescence signal, although increase of the excitation powers leads to fluorescence upon exclusive irradiation of each color. All subsequent measurements are performed at power levels where the background signal from irradiation with one color only is reduced to negligible level of percent. The absolute power levels applied to the sample for acquisition of the images shown was 15 mW at 800 nm and 0.4 mW at 400 nm.

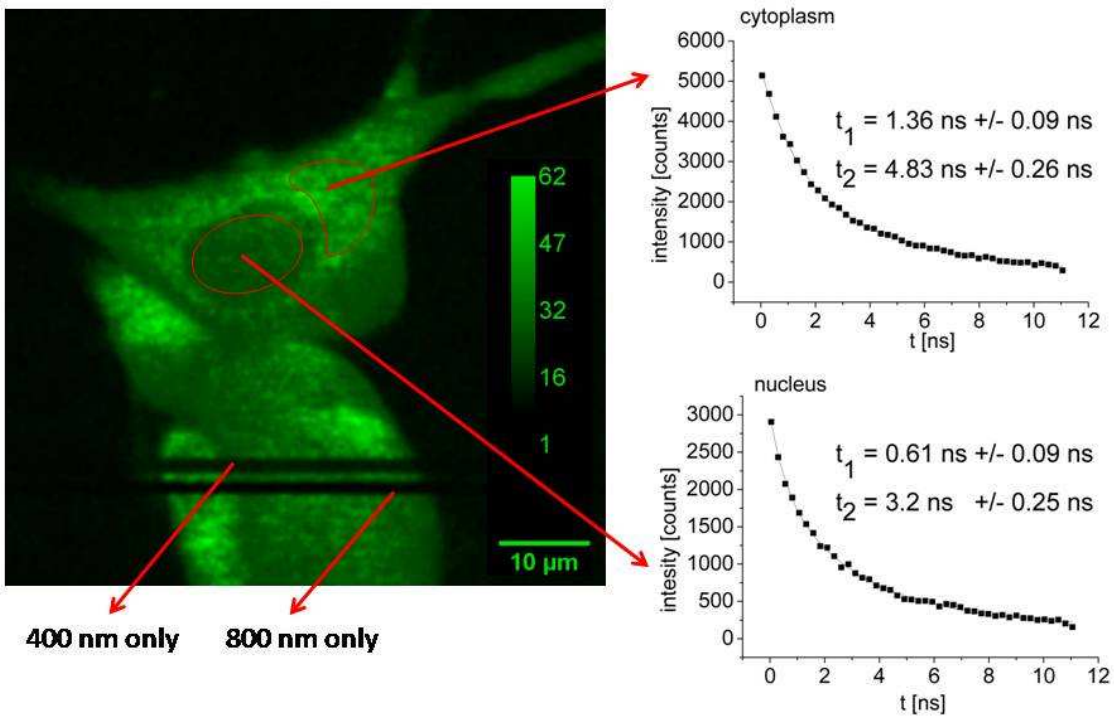

Figure 3: 2c2pLSM image of MIN6 cells. Graphs on the right show fluorescence decay data averaged over the marked areas. The red line represents a biexponential function which fits the data best. t1 and t2 are the fluorescence lifetimes corresponding to this fit. Fluorescence lifetimes in the cytoplasm are higher than in the nucleus. The dark stripes (400 nm only, 800 nm only) show that other than 2c2p absorption processes are neglectable.

For cell imaging the non-descanned detection method in combination with the sample scanner is used. Figure 3 shows a UV fluorescence image of a MIN 6 cell acquired with this setup. Fluorescence intensity is detected at 350 nm with the APD TCSPC system and integrated over all relevant time channels. In the lower quarter of this image two black stripes can be seen. In these areas one of the two excitation laser beams was blocked. The black stripes prove that practically no fluorescence was observed by one-color irradiation.

The average fluorescence decay data collected over the designated areas is shown in the diagrams to the right in figure 3. Summation over the pixels in the designated areas renders two fluorescence decay curves that are of good quality as they show only little noise. A biexponential decay was found to fit the data best. The fluorescence lifetimes in the cytoplasm are significantly longer than those found in the nucleus.

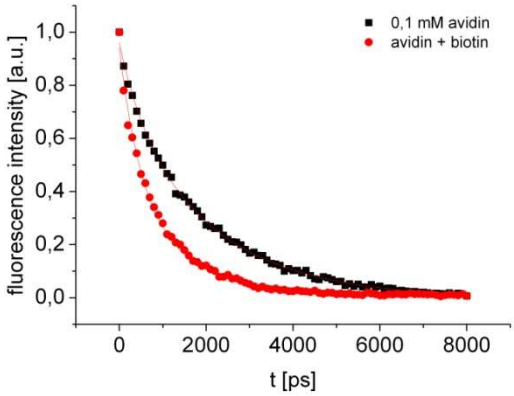

Figure 4: 2c2p excitation of avidin fluorescence. Intrinsic fluorescence lifetime of a 1mM avidin solution in PBS (black) and a solution containing 1mM avidin and 1mM biotin in PBS (red). Displayed data represent mean values of 3 measurements for avidin and avidin plus biotin, respectively. Solid lines represent a global biexponetial decay with shared decay parameters fitting the data best. Parameters are shown in table 1.

Biexponential fit	Avidin		avidin + biotin		ΔA
y0	-0.005	+/- 0.004	-0.004	+/-0.002	
A1	0,23	+/-0,03	0,69	+/-0,02	-0,46
τ1	0.55 ns	+/-0.02 ns	0.55ns	+/-0.02 ns	
A2	0,74	+/-0,02	0,26	+/-0,02	0,48
τ2	2.10 ns	+/-0.08 ns	2.10 ns	+/-0.08	

table 1: parameters of a bioexponential decay fitting the data shown in fig. 3 best. A: preexponential factor, τ: decay constant.

An example for the significance of fluorescence lifetime measurements of intrinsic protein fluorescence is shown in figure 4. Using the camera beam scanning setup as describes above (figure 1A) the binding of biotin to avidin is monitored. The data shown in figure 4 represent the fluorescence decay data of a 0.1 mM solution of avidin in PBS. The second curve represents the data collected after addition of an equimolar amount of biotin. The data was integrated over a scanning area of about 10 µm x 10 µm. A biexponential decay was found to fit the data best. Adding more biotin does not reduce the fluorescence lifetime further. Both data sets were fitted using a global least square fit with shared decay parameters. Two mean lifetimes, 0.5 ns +/- 0.02 ns for the short and 2.1 ns +/- 0.08 ns for the long lifetime component are determined with good accuracy. For avidin a ratio of the preexponential factors of the short and the long lifetime of approximately 1:3 was found. For avidin in the presence of equimolar biotin a ratio of almost 3:1 was found.

7.5 Discussion

With Figure 3 and 4 we present first applications of the concept of 2c2pLSM. The applicability of this concept is demonstrated by imaging UV fluorophores inside living cells as well as by monitoring of the biotin binding to avidin. Our results show that the fluorescence intensity generated by 2c2p excitation is sufficient for label free cell imaging and monitoring changes in intrinsic protein fluorescence lifetimes.

The cross correlation experiment performed with the microscope setup using a Zeiss plan-Neofluar 40x/1.3 oil immersion objective renders a cross correlation curve with a FWHM value of 545 fs. In previous experiments a FWHM value of 270 fs was found. This indicates a pulse broadening by a factor of 2.[54] The main difference between the two setups is that the former setup contained no lenses except one achromatic lens for focusing the beams into the sample cuvette. In the present microscope setup there are five additional lenses and one microscope objective. These optical elements are responsible for the dispersive broadening of the pulses and, hence, the cross correlation curve. This leads to the conclusion that a major improvement can be achieved by implementing a pre-chirp setup to compensate for the dispersion effects. When the pulse length of each beam is thereby reduced to its original value

an up to four times higher excitation efficiency can be expected. However, with this 2c2p setup we have for the first time an experimental setup where the pulse broadening by the objective can be measured easily.

For 2c2p imaging the intensity of each laser beam is kept so low that almost no fluorescence is detected when one laser beam is irradiated alone. This shows the advantage of relative low excitation powers of 2c2p excitation compared to those needed for three photon excitation.

Figure 4 demonstrates the possibility of imaging intrinsic protein fluorescence in living cells using 2c2pLSM. As expected, there is lower fluorescence intensity in the nucleus compared to the cytoplasm indicating different concentrations of tryptophan and, therefore, differences in protein concentration. Although from these first pictures, a detailed conclusion about the tryptophan distribution inside the imaged cells cannot be drawn, they demonstrate the possibilities for further investigations. E.g. the setup is ideally suited for performing fluorescence recovery after photo bleaching (FRAP) experiments which could yield information about the rate of protein syntheses and diffusion.[76]The difference in the fluorescence lifetime between nucleus and cytoplasm is caused by different tryptophan environments. The fluorescence lifetime of tryptophan is highly sensitive to its surrounding and many models have been proposed to explain this behavior.[29] It was found that the conformation of tryptophan has a major effect on its lifetime. Especially different angles of rotation around the bonds between the mesomeric system of tryptophan and its acidic function are proposed to have great effect on the lifetime. This kind of rotation determines the distance between the excitable π-system and the carbonyl as a possible quencher. Hence, different rotamers of tryptophan have different lifetimes. Of course other polar molecules in direct neighborhood also have great influence on the fluorescence lifetime of tryptophan as they can act as quencher.

Apart from those rather sophisticated and detailed studies on the fluorescence lifetime of tryptophan containing proteins in solution a general qualitative statement can be made:[29] short lifetimes are found when the surrounding of tryptophan allows it to rotate freely, e.g. if it is not bound or bound in a short peptide e.g. a tripeptide.[27] Long lifetimes are preferably found when tryptophan is bound in a constraining complex molecule like big proteins.[62] Therefore, it can be concluded that the fluorescence lifetime data from the nucleus reflect an excess of low molecular tryptophan whereas the longer lifetimes in the cytoplasm reflect tryptophan in a high molecular surrounding. This is in accordance with the known protein biosynthesis which takes place outside the nucleus.

Fluorescence lifetime measurements can provide detailed information about protein reactions. Figure 3 shows fluorescence decay data obtained after 2c2p excitation of the intrinsic fluorescence of avidin. The special property of avidin is, as widely known, its highly specific and strong binding to biotin. This binding mechanism has found broad application in numerous fields of biochemistry. It is used in immuno assays as well as in purification procedures. 2c2pLSM offers a minimal invasive multi photon fluorescence tool to analyze protein reactions like the avidin biotin binding without labeling. This might be a useful tool for evaluating the success of a biochemical reaction or assay, to give just one example. Due to the minimal amount of sample needed it might even be used for high troughput screening using fast evaluation methods of the fluorescence lifetime.[44, 77]

The origin of the reduction in fluorescence lifetime can be understood with respect to the crystal structure of an avidin biotin complex.[78] In total, avidin contains four tryptophans, two of which are located directly at the binding pocket of biotin. Hence, it seems very likely that the reduction in fluorescence lifetime of avidin upon binding of biotin is due to a quenching mechanism between biotin and these two tryptophans. This model is supported by the evaluation of the parameters obtained from the biexponential fit to the experimental data. The 1:3 ratio of the preexponential factor of the short and the long fluorescence lifetime can be interpreted as 1 tryptophan predominantly exhibiting a short lifetime and the other three predominantly showing a long fluorescence lifetime. The fluorescence lifetimes are considered to be predominant only and not to be the only ones because it is unlikely that these tryptophans possess only a monoexponential fluorescence intensity decay.[27, 62] Nevertheless, addition of equimolar biotin leads to a significant shift in the preexponential factors of the two lifetime components. Each preexponential factor is shifted by a difference of about 0.5. Considering the normalization of the fluorescence decay data and the four tryptophans of avidin, this is consistent with a change in fluorescence lifetime from long to short of exactly two tryptophans per avidin molecule. Similar findings have been reported earlier although the measured fluorescence lifetimes differ from our results.[79] With respect to the crystal structure, these two are most likely the tryptophans located in the biotin binding pocket whose fluorescence is quenched when biotin binds. The remaining preexponential factor of 0,25 of the long lifetime component indicates that it is one of the remote tryptophans that exhibits a long fluorescence lifetime and that the other one posseses a short fluorescence lifetime.

7.6 Conclusion

With 2c2pLSM we demonstrate a novel multi photon excitation fluorescence microscope technique that uses photons at two different wavelengths. The advantages are an extended spectral range where e.g. the Ti:Sa laser can be used for excitation and imaging of UV fluorophores, a reduced photo damage compared to one photon techniques and the possibility of performing highly resolved fluorescence microscopy with standard objectives which are not transparent at the effective excitation wavelength in the UV range. Additionally, all advantages of multi photon techniques like intrinsic 3D resolution and increased penetration depth into biological tissue also apply for 2c2pLSM. The fact, that e.g. 400 nm light is not ideal for deep tissue imaging is compensated by using higher light intensity at 800 nm and only low intensities at 400 nm.

2c2pLSM performed with 400 nm and 800 nm light is ideal for excitation of tryptophan at an effective excitation wavelength of 266 nm. With this technique the autofluorescence of MIN-6 cell was imaged. Different fluorescence lifetimes were found for nucleus and cytoplasm. To demonstrate the applicability of the method to label free protein studies the binding of biotin to avidin was monitored. From the obtained fluorescence lifetimes it can be concluded that probably two tryptophan residues which are located at the binding site of avidin are quenched by the binding of tryptophan.

Hence, 2c2pLSM can be a useful tool for non labeling protein fluorescence studies as well as for in vivo cell imaging.

7.7 References

[1] H. Shuman, J. M. Murray, C. DiLullo *Biotechniques*. **1989**, 7, 154-163.

[2] W. Denk, J. H. Strickler, W. W. Webb *Science, New Series*. **1990**, 248, 73-76.

[3] F. Helmchen, W. Denk *Nautre Methods*. **2005**, 2, 933-940.

[4] R. Heintzmann, P. A. Benedetti *Appl. Opt.* **2006**, 45, 5037-5045.

[5] D. Karadaglić, T. Wilson *Micron*. **2008**, 39, 808-818.

[6] K. I. Willig, R. R. Kellner, R. Medda, B. Hein, S. Jakobs, H. S. W. *Nature Methods*. **2006**, 3, 721-723.

[7] B. R. Rankin, R. R. Kellner, S. W. Hell *Opt. Lett.* **2008**, 33, 2491-2493.

[8] A. Egner, C. Geisler, C. v. Middendorff, H. Bock, D. Wenzel, R. Medda, M. Andresen, A. C. Stiel, S. Jakobs, C. Eggeling, A. Schönle, S. W. Hell *Biophys. J.* **2007**, 93, 3285-3290.

[9] R. Heintzmann, G. Ficz *Brief Funct Genomic Proteomic*. **2006**, 5, 289-301.

[10] P. R. Monson, W. M. McClain *J. Chem. Phys.* **1971**, 56, 4817-4825.

[11] J. R. Lakowicz, I. Gryczynsiki, H. Malak, Z. Gryczynski *Photochem. Photobiol.* **1996**, 64, 632-635.

[12] K. M. Marks, G. P. Nolan *Nature Methods*. **2006**, 3.

[13] R. Y. Tsien *Biochemistry*. **1980**, 19, 2396-2404.

[14] P. H. Hai-Jui Lin, Jung Sook Kang, Joseph R. Lakowicz. **2001**.

[15] H. S. Hai-Jui Lin, Joseph R. Lakowicz *Analytical Biochemistry*. **1999**, 269, 162-167.

[16] R. Y. Tsien *Annu Rev Biochem*. **1998**, 67, 509-544.

[17] J. M. Tavare, L. M. Fletcher, P. B. Oatey, L. Tyas, J. G. Wakefield, G. I. Welsh *Diabetic Medicine*. **2001**, 18, 253-260.

[18] A. A. H. Shaohui Huang, Watt W. Webb *Biophysical Journal*. **2002**, 82, 2811–2825.

[19] J. R. Lakowicz, Principles of fluorescence spectroscopy Kluwer Academic/Plenum Publishers, New York, **2006**.

[20] J. R. Lakowicz, I. Gryczynski *Biophys. Chem.* **1992**, 45, 1-6.

[21] M. Hellings, M. De Maeyer, S. Verheyden, Q. H. Els, J. M. Van Damme, W. J. Peumans, Y. Engelborghs *Biophys. J.* **2003**, 85, 1894-1902.

[22] A. V. Ostrovsky, L. P. Kalinichenko, V. I. Emelyanenko, A. V. Klimanov, E. A. Permyakov *Biophys. Chem.* **1987**, 30, 105-112.

[23] Y. Engelborghs *Journal of Fluorescence*. **2003**, 13, 9-16.

[24] M. K. Kuimova, G. Yahioglu, J. A. Levitt, K. Suhling *J Am Chem Soc*. **2008**, 130, 6672-6673.

[25] R. Niesner, B. Peker, P. Schlüsche, K. H. Gericke, C. Hoffmann, D. Hahne, C. Müller-Goymann *Pham Res*. **2005**, 22, 1079-1087.

[26] R. K. Benninger, Y. Koç, O. Hofmann, J. Requejo-Isidro, M. A. Neil, P. M. French, A. J. DeMello *Anal. Chem.* **2006**, 78, 2272-2278.

[27] G. R. Fleming, J. M. Morris, R. J. Robbins, G. J. Woolfe, P. J. Thistlethwaite, G. W. Robinson *Proc. Natl. Acad. Sci. USA*. **1978**, 75, 4652-4656.

[28] N. Vekshin, M. Vincent, J. Gallay *Chem. Phys. Let.* **1992**, 199, 459-464.

[29] Y. Engelborghs *Spectrochimica Acta*. **2001**, 57, 2255-2270.

[30] R. Niesner, V. Andresen, J. Neuman, H. Spieker, M. Gunzer *Biophys. J.* **2007**, 93, 2519-2529.

[31] R. Weissleder, V. Ntziachristos *Nature Medicine*. **2003**, 9, 123-128.

[32] R. Niesner, W. Roth, K.-H. Gericke *Chem. Phys. Chem.* **2004**, 5, 678-687.

[33] D. Elson, J. Requejo-Isidro, I. Munro, F. Reavell, J. Siegel, K. Suhling, P. Tadrous, R. Benninger, P. Lanigan, J. McGinty, C. Talbot, B. Treanor, S. Webb, A. Sandison, A. Wallace, D. Davis, J. Lever, M. Neil, D. Phillips, G. Stamp, P. French *Photochem. Photobiol. Sci.* **2004**, 3, 795-801.

[34] W. Becker, A. Bergmann, G. Biscotti, A. Rück *Proc. Spie.* **2004**, 5340, 1-9.

[35] E. Gratton, S. Breusegem, J. Sutin, Q. Ruan, N. Barry *Biomed. Opt.* **2003**, 8, 381-390.

[36] K. Suhling, P. M. W. French, D. Phillips *Photochem. Photobiol. Sci.* **2005**, 4, 13-22.

[37] W. M. McClain *J. Chem. Phys.* **1972**, 58, 324-326.

[38] I. Gryczynski, H. Malak, J. Lakowicz, R. *Biospec.* **1997**, 3, 97-101.

[39] J. Palero, W. Garcia, C. Saloma *Opt. Comm.* **2002**, 211, 65–71.

[40] J. Chen, K. Midorikawa *Opt. Let.* **2004**, 29, 1354.

[41] M. O. Cambaliza , C. Saloma *Opt. Comm.* **2000**, 184, 25-35.

[42] A. N. Pisarevskii, S. N. Cherenkevich, V. T. Andrianov *Zhurnal Prikladnoi Spektroskopii,*. **1966**, 5, 621-624,.

[43] P. R. Monson, W. M. McClain *J. Chem. Phys.* **1969**, 53, 29.

[44] R. Niesner, B. Peker, P. Schlüsche, K.-H. Gericke *ChemPhysChem.* **2004**, 5, 1141-1149.

[45] U. Brackmann, Lambdachrome Laser dyes, Lambda Physik GmbH, Göttingen, Germany, **1986**.

[46] R. Wijnaendts van Resand, R. Vogel, S. Provencher *Rev Sci Instrum*. **1982**, 53, 1392-1397.

[47] S. Georghiou, M. Thompson, A. K. Muikhopadhyay *Biochim. Biophysic. Act.* **1982**, 688, 441-452.

[48] H. Güsten, M. Rinke, H. O. Wirth *Appl. Phys.* **1988**, 45, 279-284

[49] L.-O. Essen *BIOspektrum*. **2006**, 12, 356.

[50] R. P. Sinha, D.-P. Häder *Photochem. Photobiol. Sci.,*. **2002**, 1, 225-236.

[51] R. M. Wiliams, D. W. Piston, W. W. Webb *FASEB J*. **1994**, 8, 804-813.

[52] C. Xu, W. Zipfel *Proc. Natl. Acad. Sci. USA, Biophysics*. **1996**, 93, 10763-10768.

[53] S. M. Potter *Curr. Biol.* **1996**, 6, 1595-1598.

[54] S. Quentmeier, S. Denicke, J.-E. Ehlers, R. A. Niesner, K.-H. Gericke *J. Phys. Chem. B.* **2008**, 112, 5768-5773.

[55] A. B. Wolfgang Becker, C. Biskup, L. Kelbauskas, T. Zimmer, N. Klöcker, K. Benndorf *Proc. Spie.* **2003**, 4963, 1-10.

[56] N. Joshi, V. O. de Joshi, S. Contreras, H. Gil, H. Medina, A. Siemiarczuk *SPIE*. **1999**, 3602, 124-131.

[57] A. V. Agronskaia, H. C. Gerritsen, L. Tertoolen *Journal of Biomedical Optics*. **2004**, 9, 1230-1337.

[58] R. K. P. Benninger, O. Hofman, J. McGinty, J. Requejo-Isidro, I. Munro, M. A. A. Neil, A. J. de Mello, P. M. W. French *Optics Express*. **2005**, 13, 6275-6285.

[59] C. C. Quentmeier, A. Wehling, P. J. Walla *Journal of Biomolecular Screening*. **2007**, 12, 2-10.

[60] E. L. Gelamo, M. Tabk *Spectrochimica Acta*. **2000**, 56, 2255-2271.

[61] J. Siegel, K. C. Benny Lee, A. Vlandas, G. L. Gambaruto, S. E. D. Webb, S. Lévêque-Fort, D. S. Elson, P. J. Tadrous, G. W. H. Stamp, A. L. Wallace, M. J. Lever, P. M. W. French. **2002**.

[62] A. Siemiarczuk, C. E. Petersen, C.-E. Ha, J. Yang, N. V. Bhagavan *Cell Biochemistry and Biophysics*. **2004**, 40, 115-122.

[63] M. J. Kronman *Biochimica et Biophysica Acta*. **1967**, 19, 19-35.

[64] G. Sanyal, L. M. Richard, K. L. Carraway, D. Puett *Biochemistry*. **1988**, 27, 6229-6236.

[65] S. J. Strickler, R. A. Berg *J. Chem. Phys.* **1962**, 37, 814-822.

[66] W. R. Zipfel, R. M. Wiliams, R. Christie, A. Y. Nikitin, B. Hyman, W. W. Webb *PNAS*. **2003**, 100, 7075-7080.

[67] D. Bird, M. Gu *Optics Letters*. **2003**, 28, 1552-1554.

[68] B. A. Flusberg, J. C. Jung, E. D. Cocker, E. P. Anderson, M. J. Schnitzer *OPTICS LETTERS*. **2005**, 30, 2272-2274.

[69] K. König, I. Riemann, A. Ehlers, R. Buckle, E. Dimitrow, M. Kaatz, J. Fluhr, P. Elsner *Proc Spie*. **2006**, 6089.

[70] C. M. Blanca, C. Saloma *Applied Optics*. **2001**, 40, 2722-2729.

[71] H. Dobrydnev *Physik. Rev.* **1995**, 52, 4010-4016.

[72] M. Lim, C. Saloma *APPLIED OPTICS*. **2003**, 42, 3398-3406.

[73] G. P. Kurzban, G. Gitlin, E. A. Bayer, M. Wilchek, P. M. Horowitz *Journal of Protein Chemistry*. **1990**, 9, 673-681.

[74] X. S. Gan, M. Gu *JOURNAL OF APPLIED PHYSICS*. **2000**, 87, 3214-3221.

[75] V. E. Centonze, J. G. White *Biophysical Journal*. **1998**, 75, 2015.

[76] A. K. Kenworthy *Methods in Molecular Biology* **2007**, 398, 179-192.

[77] S. Turconi, R. P. Bingham, U. Haupts, A. J. Pope *Journal of Biomolecular Screening*. **2001**, 12, 1-12.

[78] L. Pugliese, M. Malcovati, A. Coda, M. Bolognesi *J. Mol. Biol.* **1994**, 42, 235.
[79] G. Mei, L. Pgliese, N. Rosato, L. Toma, M. Bolognesi, Finazzi-Agrò *K. Mol. Biol.* **1994**, 242, 559-565.

Danksagung

An dieser Stelle möchte ich allen danken, die mir die Vollendung meiner Promotion ermöglichten:
Meinem Mentor Herrn Prof. Dr. Karl-Heinz Gericke möchte ich für die interessante und spannende Aufgabenstellung sowie für die vielen fachlichen Diskussionen und die herzliche Aufnahme in seine Arbeitsgruppe danken.
Für die Übernahme des Koreferats und die fachliche Kooperation bei dem BSA Projekt möchte ich Herrn Prof. Dr. Peter Jomo Walla danken.

Herrn Prof. Dr. Ingo Rustenbeck und seinem Arbeitskreis gilt mein Dank für das zur Verfügung stellen der MIN-6 Zelle sowie für die Anleitung zur Zellkultur.

Stefan Denicke und Jan-Eric Ehlers danke ich für das reibungslose Teilen des Labors und für die vielen fachlichen Diskussionen. Bei der gesamten Arbeitsgruppe möchte ich mich für die freundliche und jederzeit hilfsbereite Atmosphäre bedanken.

Mein Dank gilt desweiteren den technischen Mitarbeitern der Werkstatt sowie der Elektronik für die freundliche Unterstützung bei Spezialanfertigungen.

Ganz besonders danke ich natürlich meinen Eltern, die mir das Studium erst ermöglichten und mich jederzeit unterstützten, sowie meiner Frau Claudia, die mir bei meiner Arbeit viel Verständnis und Geduld entgegenbrachte.